Published for SISSA by Springer

Received: *June 28, 2017*
Accepted: *September 24, 2017*
Published: *October 30, 2017*

Correlators in the $\mathcal{N} = 2$ supersymmetric SYK model

Cheng Peng, Marcus Spradlin and Anastasia Volovich

Department of Physics, Brown University,
Providence RI 02912, U.S.A.

E-mail: cheng_peng@brown.edu, marcus_spradlin@brown.edu, anastasia_volovich@brown.edu

Abstract: We study correlation functions in the one-dimensional $\mathcal{N} = 2$ supersymmetric SYK model. The leading order 4-point correlation functions are computed by summing over ladder diagrams expanded in a suitable basis of conformal eigenfunctions. A novelty of the $\mathcal{N} = 2$ model is that both symmetric and antisymmetric eigenfunctions are required. Although we use a component formalism, we verify that the operator spectrum and 4-point functions are consistent with $\mathcal{N} = 2$ supersymmetry. We also confirm the maximally chaotic behavior of this model and comment briefly on its 6-point functions.

Keywords: 1/N Expansion, Extended Supersymmetry, Field Theories in Lower Dimensions, AdS-CFT Correspondence

ArXiv ePrint: 1706.06078

https://doi.org/10.1007/JHEP10(2017)202

Contents

JHEP10(2017)202

1 Introduction

Extensive studies of the Sachdev-Ye-Kitaev (SYK) model [1–6] have revealed several fascinating features of this solvable large-N model. Perhaps the most important property is its quantum chaotic behavior [4–6] that makes it a promising, but still somewhat mysterious, candidate for a holographic dual of AdS_2 quantum gravity [7–16]. The model develops an emergent (approximate) reparametrization symmetry at low energy [6, 17–19] that is also present in dilaton gravity theories on AdS_2 [6, 20–23]. It has intimate relations with well-studied random matrix models [6, 18, 24–32], it further boosts the study of a different type of the large-N limit [33–48], and it is closely related to vector models [49]. The SYK model can be generalized to include extra symmetries [50] or to live in higher dimensions [51–56]. Of course, the model is also of great interest in condensed matter physics [51, 54, 57–67]. Other related recent work can be found in [68–83].

In particular, supersymmetric extensions of the SYK model have been constructed in [84], and a supersymmetric SYK-like model without a random coupling has been proposed in [41]. Aspects of supersymmetric SYK models have also been studied in [31, 50, 85, 86]. In this paper, we study the correlation functions of the $\mathcal{N} = 2$ supersymmetric SYK model proposed in [84]. One nice feature of the $\mathcal{N} = 2$ model, compared to its $\mathcal{N} = 1$

cousin, is that the supersymmetry is preserved not only in the large-N limit, but also for finite N [84].

In section 2 we review the $\mathcal{N} = 2$ model, which has a few new technical features compared to the $\mathcal{N} = 1$ theory. In section 3 we discuss the fact that in contrast to both the fermionic SYK model studied in [4–6] and the $\mathcal{N} = 1$ supersymmetric model studied in [84], the computation of 4-point functions in the $\mathcal{N} = 2$ model requires both antisymmetric and symmetric conformal eigenfunctions, which we work out. In section 4 we compute the 4-point functions and see another difference: divergences in 4-point functions arise from the exchange of a full $\mathcal{N} = 2$ supermultiplet. This $\mathcal{N} = 2$ supermultiplet presumably leads to a super-Schwarzian effective action due to the breaking of conformal symmetry in the infared. While these new features were anticipated [84], we provide some concrete computations to confirm them. Finally in section 5 we briefly comment on the operator product expansion (OPE) between operators that are bilinear in the fundamental fields. These OPE coefficients may be extracted from our 4-point function results in a manner almost identical to the analysis of [32].

Note added. As we were preparing this work for submission we became aware of other work [87, 88] on supersymmetric SYK models. Among many other things, the paper [87] studies the correlation functions of the $\mathcal{N} = 1$ supersymmetric SYK model using the formalism of a real superfield. In this work we focus on the $\mathcal{N} = 2$ supersymmetric SYK model which could be constructed using a complex superfield, although we use component fields. Our paper therefore also overlaps with the newly appearing paper [89] on the SYK model with complex fermions.

2 The operator spectrum

In this paper we study the $\mathcal{N} = 2$ supersymmetric SYK model of [84]. We begin in this section by supplying some details about the spectrum of this model that were not given explicitly in [84]. The model describes N complex fermions ψ_i in 1+0 dimensions governed by the Lagrangian

$$\mathcal{L} = i\bar{\psi}_i\partial\psi_i - \bar{b}_i b_i + i^{\frac{q-1}{2}} C_{ij_1\ldots j_{q-1}}\bar{b}_i\psi_{j_1}\ldots\psi_{j_{q-1}} + i^{\frac{q-1}{2}}\bar{C}_{ij_1\ldots j_{q-1}} b_i\bar{\psi}_{j_1}\ldots\bar{\psi}_{j_{q-1}}\,, \tag{2.1}$$

where b is a complex bosonic auxiliary field, q is an odd integer (so that the Lagrangian is bosonic), and $C_{i_1\ldots i_q}$ is a random complex coupling drawn from a Gaussian distribution with

$$\langle C_{i_i\ldots i_q}\bar{C}_{i_i\ldots i_q}\rangle = \frac{(q-1)!\,J}{N^{q-1}}\,. \tag{2.2}$$

We are interested in the large-N limit, with J held fixed.

2.1 2-point functions

We begin by considering the 2-point functions

$$G^{\psi}(\tau_{12}) = \frac{1}{N}\sum_{i=1}^{N}\langle\psi_i(\tau_1)\bar{\psi}_i(\tau_2)\rangle\,, \qquad G^{b}(\tau_{12}) = \frac{1}{N}\sum_{i=1}^{N}\langle b_i(\tau_1)\bar{b}_i(\tau_2)\rangle \tag{2.3}$$

in Euclidean time τ, where we use $\tau_{ij} = \tau_i - \tau_j$. The complex conjugate 2-point functions, obtained by replacing $\psi \leftrightarrow \bar{\psi}$ and $b \leftrightarrow b$, evidently satisfy

$$G^{\bar{\psi}}(\tau) = -G^{\psi}(-\tau)\,, \qquad G^{\bar{b}}(\tau) = G^{b}(-\tau)\,. \tag{2.4}$$

In the IR limit, the Schwinger-Dyson equations relating the 2-point functions to the corresponding self-energies read

$$\Sigma^{\psi}(\tau_{12}) = (q-1)JG^{b}(\tau_{12})\big(G^{\bar{\psi}}(\tau_{12})\big)^{q-2}, \tag{2.5}$$

$$\Sigma^{b}(\tau_{12}) = J\big(G^{\psi}(\tau_{12})\big)^{q-1}, \tag{2.6}$$

$$-\delta(\tau_{13}) = \int d\tau_2\, G^{\psi}(\tau_{12})\Sigma^{\psi}(\tau_{23})\,, \tag{2.7}$$

$$-\delta(\tau_{13}) = \int d\tau_2\, G^{b}(\tau_{12})\Sigma^{b}(\tau_{23})\,, \tag{2.8}$$

together with their complex conjugates. Taking the ansatz

$$G^{b}(\tau_{12}) = \frac{b_b}{|\tau_{12}|^{2\Delta_b}}\,, \qquad G^{\psi}(\tau_{12}) = \frac{b_\psi\,\mathrm{sgn}(\tau_{12})}{|\tau_{12}|^{2\Delta_\psi}}\,, \tag{2.9}$$

the solution is found to be [84]

$$\Delta_\psi = \frac{1}{2q}\,, \qquad \Delta_b = \frac{1+q}{2q}\,, \qquad b_\psi = \left(\frac{\tan\frac{\pi}{2q}}{2\pi J}\right)^{1/q}, \qquad b_b = \frac{1}{q}\left(\frac{\tan\frac{\pi}{2q}}{2\pi J}\right)^{1/q}. \tag{2.10}$$

From these results and the relation (2.4) we see that

$$G^{\psi}(\tau) = G^{\bar{\psi}}(\tau)\,, \qquad G^{b}(\tau) = G^{\bar{b}}(\tau)\,. \tag{2.11}$$

2.2 The diagonal 4-point kernel

In the large-N limit, the connected 4-point functions are dominated by ladder diagrams. This will be the topic of section 4; here we only need to recall that these can be generated iteratively by repeated convolution with an appropriate integral kernel. The kernels of the different types of 4-point functions can be worked out straightforwardly. For $\langle\psi_i(\tau_1)b_i(\tau_2)\bar{\psi}_j(\tau_3)\bar{b}_j(\tau_4)\rangle$ the kernel is (see figure 1)

$$K^{d} = J(q-1)G^{\psi}(\tau_{14})G^{b}(\tau_{23})\big(G^{\psi}(\tau_{34})\big)^{q-2}, \tag{2.12}$$

where the factor of $q-1$ arises from the $(q-1)!$ in (2.2) divided by a symmetry factor $(q-2)!$. The superscript "d" indicates that this kernel is diagonal in the sense that the directions of the arrows on the left and right sides of the kernel match. This means it can be iterated directly to build ladder diagrams with arbitrarily many rungs. The operators running in the OPE channel of this kernel take the schematic form $\psi_i\partial^n b_i$, and have U(1) charge $\frac{1}{q} + \frac{q-1}{q} = 1$.

There is another kernel which is almost the same as this, but with all fields replaced by their conjugates. We could call this $K^{\bar{d}}$, but it follows from eq. (2.11) that $K^{\bar{d}} = K^{d}$.

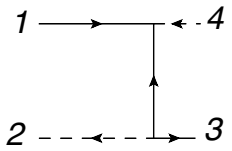

Figure 1. Kernel of the $\langle \psi_i(\tau_1) b_i(\tau_2) \bar{\psi}_j(\tau_3) \bar{b}_j(\tau_4) \rangle$ correlation. Iterating this kernel generates all ladder diagrams, which dominate the large-N limit of the connected 4-point function.

This simply means that there is another set of conjugate operators $\bar{\psi}_i \partial^n \bar{b}_i$ with the same dimensions as the ones corresponding to the kernel K^d.

In the conformal limit the kernel becomes simply

$$K_c^d(\tau_1, \tau_2; \tau_3, \tau_4) = \frac{\alpha \, \mathrm{sgn}(\tau_{14}) \, \mathrm{sgn}(\tau_{34})}{|\tau_{14}|^{1/q} |\tau_{34}|^{(q-2)/q} |\tau_{23}|^{(1+q)/q}} \,, \tag{2.13}$$

where

$$\alpha = \frac{q-1}{q} \frac{\tan(\frac{\pi}{2q})}{2\pi} \,. \tag{2.14}$$

Next we consider the kernel convolution eigen-equation

$$k \, f(\tau_1, \tau_2) = \int d\tau_3 \, d\tau_4 \, K(\tau_1, \tau_2; \tau_3, \tau_4) f(\tau_3, \tau_4) \,, \tag{2.15}$$

which for a generic kernel admits both symmetric and antisymmetric eigenfunctions $f(\tau_1, \tau_2)$. We will denote the symmetric and antisymmetric eigenvalues of the kernel (2.13) by $k_c^{s,d}$ and $k_c^{a,d}$, respectively. Here, and in all that follows, the superscripts "s" and "a" stand respectively for symmetric and antisymmetric, the subscript "c" reminds us that we are working in the conformal limit, and the superscript "d" indicates that these are the eigenvalues of the diagonal kernel K^d.

As described in section 3.2.3 of [6], conformal invariance effectively allows the eigenvalues to be determined simply by

$$k_c^{s,d} = \int d\tau_3 \, d\tau_4 \, K_c^d(1, 0; \tau_3, \tau_4) \frac{1}{|\tau_{34}|^{\Delta_\psi + \Delta_b - h}} \,, \tag{2.16}$$

$$k_c^{a,d} = \int d\tau_3 \, d\tau_4 \, K_c^d(1, 0; \tau_3, \tau_4) \frac{\mathrm{sgn}(\tau_{34})}{|\tau_{34}|^{\Delta_\psi + \Delta_b - h}} \tag{2.17}$$

in terms of a conformal weight h. Note that in this case the two outgoing lines are a boson and a fermion, so we use $\Delta_\psi + \Delta_b - h$ in the eigenfunction instead of $2\Delta_\psi - h$ as in [6]. Plugging in eqs. (2.9) and (2.10), the eigen-equations become

$$k_c^{s,d} = \alpha \int d\tau_3 \, d\tau_4 \frac{\mathrm{sgn}(1-\tau_4)}{|1-\tau_4|^{1/q} \, |\tau_3|^{(1+q)/q}} \frac{\mathrm{sgn}(\tau_{34})}{|\tau_{34}|^{\frac{3q-2}{2q} - h}} \tag{2.18}$$

$$k_c^{a,d} = \alpha \int d\tau_3 \, d\tau_4 \frac{\mathrm{sgn}(1-\tau_4)}{|1-\tau_4|^{1/q} \, |\tau_3|^{(1+q)/q}} \frac{1}{|\tau_{34}|^{\frac{3q-2}{2q} - h}} \,. \tag{2.19}$$

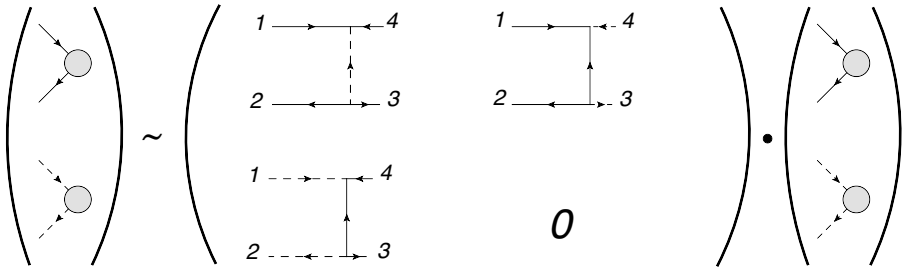

Figure 2. Kernels of the $\langle\psi_i(\tau_1)\bar{\psi}_i(\tau_2)\psi_j(\tau_3)\bar{\psi}_j(\tau_4)\rangle$, $\langle\psi_i(\tau_1)\bar{\psi}_i(\tau_2)b_j(\tau_3)\bar{b}_j(\tau_4)\rangle$, $\langle b_i(\tau_1)\bar{b}_i(\tau_2)\psi_j(\tau_3)\bar{\psi}_j(\tau_4)\rangle$ and $\langle b_i(\tau_1)\bar{b}_i(\tau_2)b_j(\tau_3)\bar{b}_j(\tau_4)\rangle$ correlation functions. Iterating these kernels to build ladder diagrams amounts to 2×2 matrix multiplication.

Using the integrals tabulated in appendix A one finds that the eigenvalues are given by

$$k_c^{s,d}(h) = \frac{\alpha\,\pi^2\cos\left(\pi(\frac{q+2}{4q}-\frac{h}{2})\right)\Gamma\left(\frac{q+2}{2q}-h\right)}{\sin\left(\frac{\pi}{2q}\right)\Gamma\left(\frac{1}{q}\right)\cos\left(\frac{\pi(1+q)}{2q}\right)\Gamma\left(\frac{1+q}{q}\right)\sin\left(\pi(\frac{3q-2}{4q}-\frac{h}{2})\right)\Gamma\left(\frac{3q-2}{2q}-h\right)}\,, \tag{2.20}$$

$$k_c^{a,d}(h) = \frac{\alpha\,\pi^2\sin\left(\pi(\frac{q+2}{4q}-\frac{h}{2})\right)\Gamma\left(\frac{q+2}{2q}-h\right)}{\sin\left(\frac{\pi}{2q}\right)\Gamma\left(\frac{1}{q}\right)\cos\left(\frac{\pi(1+q)}{2q}\right)\Gamma\left(\frac{1+q}{q}\right)\cos\left(\pi(\frac{3q-2}{4q}-\frac{h}{2})\right)\Gamma\left(\frac{3q-2}{2q}-h\right)}\,. \tag{2.21}$$

These expressions are easily seen to be in complete agreement with eq. (6.2) of [84].

2.3 The non-diagonal 4-point kernels

It is similarly easy to work out kernels corresponding to pairs of bosons or fermions on the same side of the ladder. These kernels have the property that the two legs on the left are different than the two legs on the right, so adding any additional such rung to a ladder will change the "end" of the latter. These kernels are therefore assembled into a 2×2 matrix, as illustrated in figure 2.

The entries of this kernel matrix K^{ij} are

$$K^{11} = J\frac{(q-1)!}{(q-3)!}G^{\psi}(\tau_{14})G^{\bar{\psi}}(\tau_{23})G^{\bar{b}}(\tau_{34})\left(G^{\psi}(\tau_{34})\right)^{q-3}, \tag{2.22}$$

$$K^{12} = J\frac{(q-1)!}{(q-2)!}G^{\psi}(\tau_{14})G^{\bar{\psi}}(\tau_{23})\left(G^{\psi}(\tau_{34})\right)^{q-2}, \tag{2.23}$$

$$K^{21} = J\frac{(q-1)!}{(q-2)!}G^{\bar{b}}(\tau_{14})G^{b}(\tau_{23})\left(G^{\psi}(\tau_{34})\right)^{q-2}, \tag{2.24}$$

with $K^{22}=0$ since there is no connected contribution to $\langle b_i(\tau_1)\bar{b}_i(\tau_2)b_j(\tau_3)\bar{b}_j(\tau_4)\rangle$. We now repeat the computation of eqs. (2.16) and (2.17) to find the eigenvalues k^{ij} of the three K^{ij}. In the conformal limit we have from eqs. (2.9) and (2.10) that

$$\begin{aligned}
K_c^{11} &= \frac{(q-2)\alpha\,\mathrm{sgn}(\tau_{14})\,\mathrm{sgn}(\tau_{23})}{|\tau_{14}|^{1/q}|\tau_{34}|^{(q-3)/q}|\tau_{34}|^{(q+1)/q}|\tau_{23}|^{1/q}}\,,\\
K_c^{12} &= \frac{q\alpha\,\mathrm{sgn}(\tau_{14})\,\mathrm{sgn}(\tau_{23})\,\mathrm{sgn}(\tau_{34})}{|\tau_{14}|^{1/q}|\tau_{34}|^{(q-2)/q}|\tau_{23}|^{1/q}}\,,\\
K_c^{21} &= \frac{\frac{\alpha}{q}\,\mathrm{sgn}(\tau_{34})}{|\tau_{14}|^{(1+q)/q}|\tau_{34}|^{(q-2)/q}|\tau_{23}|^{(1+q)/q}}\,.
\end{aligned} \tag{2.25}$$

As in the diagonal case, the eigenfunctions can be either symmetric or antisymmetric, and we compute them separately.

Here it is important to clarify that we call a 2-component eigenfunction of the kernel matrix "symmetric" or "antisymmetric" according to the symmetry property of only the first, fermionic component. The second, bosonic component must have the opposite symmetry, since the off-diagonal kernel entries K_c^{12} and K_c^{21} are odd under a simultaneous flip of $\tau_1 \leftrightarrow \tau_2$ and $\tau_3 \leftrightarrow \tau_4$.

To find the antisymmetric eigenvalues we therefore consider a 2-component trial eigenfunction of the form

$$\begin{pmatrix} \dfrac{\mathrm{sgn}(\tau_{34})}{|\tau_{34}|^{\frac{1}{q}-h}} & \dfrac{1}{|\tau_{34}|^{\frac{q+1}{q}-h}} \end{pmatrix}. \tag{2.26}$$

As in the previous subsection the powers in the denominator are taken in consideration of the dimensions of the free legs in the associated kernel diagram, in this case $2\Delta_\psi$ and $2\Delta_b$, respectively. When acting on a vector of this form, we find that the kernel has the non-zero matrix elements

$$k_c^{a,11} = \frac{-(q-2)\alpha\pi^2 \sin\left(\pi(\frac{1}{2q}-\frac{h}{2})\right)\Gamma\left(\frac{1}{q}-h\right)}{\sin\left(\frac{\pi}{2q}\right)^2\Gamma\left(\frac{1}{q}\right)^2 \sin\left(\pi(\frac{2q-1}{2q}-\frac{h}{2})\right)\Gamma\left(\frac{2q-1}{q}-h\right)}\,, \tag{2.27}$$

$$k_c^{a,12} = \frac{-q\alpha\,\pi^2 \sin\left(\pi(\frac{1}{2q}-\frac{h}{2})\right)\Gamma\left(\frac{1}{q}-h\right)}{\sin\left(\frac{\pi}{2q}\right)^2\Gamma\left(\frac{1}{q}\right)^2 \sin\left(\pi(\frac{2q-1}{2q}-\frac{h}{2})\right)\Gamma\left(\frac{2q-1}{q}-h\right)}\,, \tag{2.28}$$

$$k_c^{a,21} = \frac{\frac{\alpha}{q}\pi^2 \cos\left(\pi(\frac{q+1}{2q}-\frac{h}{2})\right)\Gamma\left(\frac{q+1}{q}-h\right)}{\cos\left(\pi\frac{q+1}{2q}\right)^2\Gamma\left(\frac{q+1}{q}\right)^2 \cos\left(\pi(\frac{q-1}{2q}-\frac{h}{2})\right)\Gamma\left(\frac{q-1}{q}-h\right)}\,. \tag{2.29}$$

The two eigenvalues of the 2×2 matrix $k_c^{a,ij}$ can be represented as[1]

$$k^{a,\pm}(h) = \mp\frac{\Gamma(2-\frac{1}{q})\Gamma(1-\frac{h}{2}-\frac{1}{2q})\Gamma(\frac{1}{2q}+\frac{h}{2})\Gamma(\frac{1}{2}-h+\frac{1}{q}\mp\frac{1}{2})}{\Gamma(1+\frac{1}{q})\Gamma(1+\frac{h}{2}-\frac{1}{2q})\Gamma(\frac{1}{2q}-\frac{h}{2})\Gamma(\frac{3}{2}-h-\frac{1}{q}\mp\frac{1}{2})}\,. \tag{2.30}$$

It can be checked that

$$k_c^{a,+}\left(h-\frac{1}{2}\right) = k_c^{a,d}(h) \qquad \text{and} \qquad k_c^{a,-}\left(h+\frac{1}{2}\right) = k_c^{s,d}(h)\,, \tag{2.31}$$

in accord with the statement on page 30 of [84].

Similarly, to find the symmetric eigenvalues we act with the kernel on

$$\begin{pmatrix} \dfrac{1}{|\tau_{34}|^{\frac{1}{q}-h}} & \dfrac{\mathrm{sgn}(\tau_{34})}{|\tau_{34}|^{\frac{q+1}{q}-h}} \end{pmatrix} \tag{2.32}$$

[1]The eigenvalues can also be represented as $\widetilde{k}_c^{a,\pm} = \frac{1}{2}k_c^{a,11} \pm \sqrt{\frac{1}{4}(k_c^{a,11})^2 + k_c^{a,12}k_c^{a,21}}$. We caution the reader that although the sets $\{\widetilde{k}_c^{a,+}, \widetilde{k}_c^{a,-}\}$ and $\{k_c^{a,+}, k_c^{a,-}\}$ are the same for all h, it is not true that $\widetilde{k}_c^{a,\pm} = k_c^{a,\pm}$ for all h.

to find the matrix elements

$$k_c^{s,11} = \frac{(q-2)\alpha\,\pi^2 \cos\left(\pi(\frac{1}{2q}-\frac{h}{2})\right)\Gamma\left(\frac{1}{q}-h\right)}{\sin\left(\frac{\pi}{2q}\right)^2\Gamma\left(\frac{1}{q}\right)^2\cos\left(\pi(\frac{2q-1}{2q}-\frac{h}{2})\right)\Gamma\left(\frac{2q-1}{q}-h\right)}\,, \tag{2.33}$$

$$k_c^{s,12} = \frac{q\alpha\,\pi^2 \cos\left(\pi(\frac{1}{2q}-\frac{h}{2})\right)\Gamma\left(\frac{1}{q}-h\right)}{\sin\left(\frac{\pi}{2q}\right)^2\Gamma\left(\frac{1}{q}\right)^2\cos\left(\pi(\frac{2q-1}{2q}-\frac{h}{2})\right)\Gamma\left(\frac{2q-1}{q}-h\right)}\,, \tag{2.34}$$

$$k_c^{s,21} = \frac{-\frac{\alpha}{q}\pi^2 \sin\left(\pi(\frac{q+1}{2q}-\frac{h}{2})\right)\Gamma\left(\frac{q+1}{q}-h\right)}{\cos\left(\pi\frac{1+q}{2q}\right)^2\Gamma\left(\frac{1+q}{q}\right)^2\sin\left(\pi(\frac{q-1}{2q}-\frac{h}{2})\right)\Gamma\left(\frac{q-1}{q}-h\right)}\,, \tag{2.35}$$

and the corresponding eigenvalues (footnote 1 applies again)

$$k_c^{s,\pm}(h) = \mp\frac{\Gamma(2-\frac{1}{q})\Gamma(\frac{1}{2}-\frac{h}{2}-\frac{1}{2q})\Gamma(\frac{1}{2}+\frac{h}{2}+\frac{1}{2q})\Gamma(\frac{1}{2}-h+\frac{1}{q}\mp\frac{1}{2})}{\Gamma(1+\frac{1}{q})\Gamma(\frac{1}{2}+\frac{h}{2}-\frac{1}{2q})\Gamma(\frac{1}{2}-\frac{h}{2}+\frac{1}{2q})\Gamma(\frac{3}{2}-h-\frac{1}{q}\mp\frac{1}{2})}\,. \tag{2.36}$$

Notice that

$$k_c^{s,+}\left(h-\frac{1}{2}\right) = k_c^{s,d}(h) \qquad \text{and} \qquad k_c^{s,-}\left(h+\frac{1}{2}\right) = k_c^{a,d}(h)\,, \tag{2.37}$$

again in accord with [84].

It should not be a surprise to have found in eq. (2.31) that $k_c^{a,-}$ can be related to $k_c^{s,d}$ instead of to $k_c^{a,d}$: this is a consequence of the different symmetry properties of the two entries in (2.26). The relation (2.37) between $k_c^{s,-}$ and $k_c^{a,d}$ occurs for the same reason.

For a given kernel K, the dimensions of the operators running in the OPE channel of K are the values of h for which the eigenvalue(s) of K satisfy $k(h) = 1$. From the relation (2.31) between the diagonal and non-diagonal 4-point kernels, it is natural to expect that operators whose dimensions arise from the $k_c^{a,+}(h)$, $k_c^{a,d}(h)$ and $k_c^{s,-}(h)$ eigenvalues assemble into a tower of $\mathcal{N}=2$ supermultiplets with dimensions $\{h-\frac{1}{2}, h, h+\frac{1}{2}\}$. For example, for $q=3$ we have

$$k_c^{a,+}(h)=1 \quad \Rightarrow \quad h_m^{a,+} = 1,\ 3.0659,\ 5.09488,\ 7.11311,\ 9.12623,\ \ldots \tag{2.38}$$

$$k_c^{a,d}(h)=1 \quad \Rightarrow \quad h_m^{a,d} = 1.5,\ 3.5659,\ 5.59488,\ 7.61311,\ 9.62623,\ \ldots \tag{2.39}$$

$$k_c^{s,-}(h)=1 \quad \Rightarrow \quad h_m^{s,-} = 2,\ 4.0659,\ 6.09488,\ 8.11311,\ 10.1262,\ \ldots \tag{2.40}$$

in agreement with eq. (6.3) of [84]. These eigenvalues and dimensions are shown in figure 3a.

Similarly, the dimensions from the $k_c^{s,+}(h)$, $k_c^{s,d}(h)$ and $k_c^{a,-}(h)$ eigenvalues comprise a second tower of $\mathcal{N}=2$ supermultiplets. The dimensions of these eigenvalues at $q=3$ are

$$k_c^{s,+}(h)=1 \quad \Rightarrow \quad h_m^{s,+} = 1,\ 2.82114,\ 4.74091,\ 6.69332,\ 8.66092,\ \ldots \tag{2.41}$$

$$k_c^{s,d}(h)=1 \quad \Rightarrow \quad h_m^{s,d} = 1.5,\ 3.32114,\ 5.24091,\ 7.19332,\ 9.16092,\ \ldots \tag{2.42}$$

$$k_c^{a,-}(h)=1 \quad \Rightarrow \quad h_m^{a,-} = 2,\ 3.82114,\ 5.74091,\ 7.69332,\ 9.66092,\ \ldots \tag{2.43}$$

again in agreement with [84]. These eigenvalues and dimensions are shown in figure 3b.

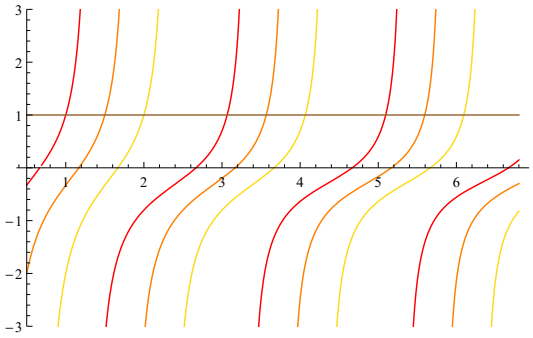

(a) The red, orange and yellow curves represent the eigenvalues $k_c^{a,+}(h)$, $k_c^{a,d}(h)$ and $k_c^{s,-}(h)$ respectively.

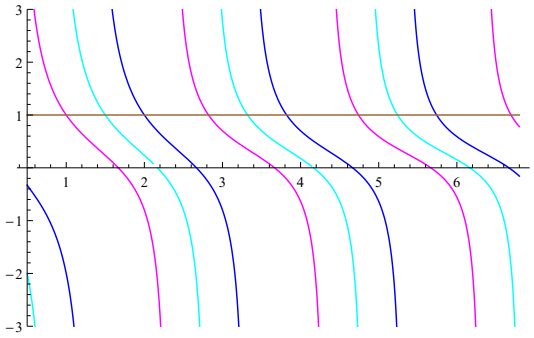

(b) The magenta, cyan and blue curves represent the eigenvalues $k_c^{s,+}(h)$, $k_c^{s,d}(h)$ and $k_c^{a,-}(h)$ respectively.

Figure 3. A plot of the eigenvalues for the $q = 3$ model. Each figure illustrates one tower of $\mathcal{N} = 2$ supermultiplets. Their intersects with the horizontal $k = 1$ line give the dimensions of operators running in the OPE channel.

2.4 The chaotic behavior

The chaotic behavior of this model can be studied in a similar way by analyzing the retarded kernels. In this subsection we carry out this analysis, partly also as a double check of our computations in the previous subsections.

The chaotic behavior is measured by out-of-time-order correlators [4, 5], which can be obtained either from an analytic continuation of the Euclidean 4-point function or directly from analyzing the retarded kernel. We take the latter approach, following [4, 5] and section 3.6.1 of [6]. The retarded kernel is defined on a complex time contour with two real time folds on two antipodal points on the thermal circle. It can expressed in terms of the retarded and ladder rung propagators

$$G_R^{\psi}(t) = 2\cos(\pi\Delta_\psi) b_\psi \left(\frac{\pi}{\beta \sinh\left(\frac{\pi t}{\beta}\right)}\right)^{2\Delta_\psi} \Theta(t)\,, \tag{2.44}$$

$$G_R^{b}(t) = -2i\sin(\pi\Delta_b) b_b \left(\frac{\pi}{\beta \sinh\left(\frac{\pi t}{\beta}\right)}\right)^{2\Delta_b} \Theta(t)\,, \tag{2.45}$$

$$G_{lr}^{x}(t) = b_x \left(\frac{\pi}{\beta \cosh(\frac{\pi t}{\beta})}\right)^{2\Delta_x}, \qquad x \in \{\psi, b\}\,, \tag{2.46}$$

which are obtained from the Euclidean propagators by analytic continuation [6, 49].

The retarded kernel contributions to the 4-point functions shown in figure 2 are

$$K_R^{11} = J\frac{(q-1)!}{(q-3)!} G_R^{\psi}(t_{14}) G_R^{\bar{\psi}}(t_{23}) G_{lr}^{b}(t_{34}) \left(G_{lr}^{\psi}(t_{34})\right)^{q-3}, \tag{2.47}$$

$$K_R^{12} = -J\frac{(q-1)!}{(q-2)!} G_R^{\psi}(t_{14}) G_R^{\bar{\psi}}(t_{23}) \left(G_{lr}^{\psi}(t_{34})\right)^{q-2}, \tag{2.48}$$

$$K_R^{21} = J\frac{(q-1)!}{(q-2)!} G_R^{\bar{b}}(t_{14}) G_R^{b}(t_{23}) \left(G_{lr}^{\psi}(t_{34})\right)^{q-2}. \tag{2.49}$$

JHEP10(2017)202

We have included a factor of i^2 in each case due to the vertex insertion on the Lorentzian time folds, and we have also included a factor of -1 on the kernels K_R^{11}, K_R^{21} arising from the operator ordering required by the contour [49]. When acting by matrix multiplication and convolution on an ansatz of the form

$$\begin{pmatrix} \frac{e^{-h\frac{\pi}{\beta}(t_1+t_2)}}{\left(\frac{\beta}{\pi}\cosh\frac{\pi t_{12}}{\beta}\right)^{\frac{1}{q}-h}} & \frac{e^{-h\frac{\pi}{\beta}(t_1+t_2)}}{\left(\frac{\beta}{\pi}\cosh\frac{\pi t_{12}}{\beta}\right)^{\frac{1+q}{q}-h}} \end{pmatrix}, \tag{2.50}$$

the nonzero matrix elements of the kernel can be explicitly evaluated as

$$k_R^{11} = 4(q-2)\alpha \frac{\cos^2\left(\frac{\pi}{2q}\right)\Gamma\left(\frac{q-1}{q}\right)^2\Gamma\left(\frac{1}{q}-h\right)}{\Gamma\left(2-h-\frac{1}{q}\right)}, \tag{2.51}$$

$$k_R^{12} = -4q\alpha \frac{\cos^2\left(\frac{\pi}{2q}\right)\Gamma\left(\frac{q-1}{q}\right)^2\Gamma\left(\frac{1}{q}-h\right)}{\Gamma\left(2-h-\frac{1}{q}\right)}, \tag{2.52}$$

$$k_R^{21} = -4\frac{\alpha}{q} \frac{\cos^2\left(\frac{\pi}{2q}\right)\Gamma\left(-\frac{1}{q}\right)^2\Gamma\left(1+\frac{1}{q}-h\right)}{\Gamma\left(1-h-\frac{1}{q}\right)}. \tag{2.53}$$

The two eigenvalues of the matrix k_R^{ij} are

$$k_R^{\pm}(h) = \mp \frac{\Gamma\left(2-\frac{1}{q}\right)\Gamma\left(\frac{1}{2}-h+\frac{1}{q}\pm\frac{1}{2}\right)}{\Gamma\left(1+\frac{1}{q}\right)\Gamma\left(\frac{3}{2}-h-\frac{1}{q}\pm\frac{1}{2}\right)}. \tag{2.54}$$

The eigenvalue k_R^- reaches its resonance value $k_R^-(h) = 1$ at $h = -1$. This indicates chaos: the eigenfunctions (2.50) grow exponentially with maximal Lyapunov parameter

$$\lambda_L = \frac{2\pi}{\beta}. \tag{2.55}$$

There are no other negative values of h that set any of the eigenvalues to one. Therefore there is no "subleading" chaotic behavior.

3 Symmetric and antisymmetric conformal eigenfunctions

The simplest way of summing ladder diagrams to evaluate a 4-point function is to first expand the 0-rung ladder diagram in a complete basis of eigenfunctions of the kernels. It is then straightforward to generate the L-rung ladder, and then to sum all ladder diagrams, since the kernels act (by convolution) diagonally in this basis. Furthermore one can make efficient use of conformal symmetry, which effectively reduces all 4-point calculations to functions of a single cross-ratio χ. In this section, which follows closely section 3.2 of [6], we determine the complete set of conformal eigenfunctions of the various ladder kernels. Particular importance is played by the transformation $\chi \to \frac{\chi}{\chi-1}$ which is a symmetry of both the fermionic SYK model studied in [4–6] and the $\mathcal{N} = 1$ supersymmetric model studied in [84, 87]. However, in our study of the $\mathcal{N} = 2$ model we will also require eigenfunctions that are antisymmetric under $\chi \to \frac{\chi}{\chi-1}$.

It is straightforward to check that the kernels commute with the conformal Casimir operator, which reads

$$\mathcal{C} = \chi^2(1-\chi)\partial_\chi^2 - \chi^2\partial_\chi \tag{3.1}$$

in terms of the conformal cross ratio

$$\chi = \frac{\tau_{12}\tau_{34}}{\tau_{13}\tau_{24}}\,. \tag{3.2}$$

It admits a set of eigenfunctions $\Phi_h(\chi)$, with eigenvalues $h(h-1)$, that satisfy

$$\mathcal{C}\Phi_h(\chi) = h(h-1)\Phi_h(\chi)\,. \tag{3.3}$$

This is an equation of hypergeometric type that for $0<\chi<1$ has two linearly independent solutions

$$F_1(\chi) = \frac{\chi^h\Gamma(h)^2}{\Gamma(2h)}\,{}_2F_1(h,h;2h;\chi)\,, \tag{3.4}$$

$$F_2(\chi) = \frac{\chi^{1-h}\Gamma(1-h)^2}{\Gamma\big(2(1-h)\big)}\,{}_2F_1(1-h,1-h;2-2h;\chi) \tag{3.5}$$

related by $h\to 1-h$, where we have chosen an overall normalization for later convenience. These expressions are useful because they manifest the behaviors χ^h, χ^{1-h} of the eigenfunctions near $\chi=0$, but it is more convenient to work in a different basis of solutions where the symmetry properties under the transformation $\chi\to\frac{\chi}{\chi-1}$ are manifest. We will denote the eigenfunctions that are symmetric and antisymmetric under this transformation by $\Phi_h^s(\chi)$ and $\Phi_h^a(\chi)$, respectively.

In the region $\chi>1$, the two solutions with definite parity under $\chi\to\frac{\chi}{\chi-1}$ are

$$\Phi^s_{\chi>1}(\chi) = \frac{\Gamma\big(\frac{1}{2}-\frac{h}{2}\big)\Gamma\big(\frac{h}{2}\big)}{\sqrt{\pi}}\,{}_2F_1\left(\frac{h}{2},\frac{1-h}{2},\frac{1}{2},\frac{(\chi-2)^2}{\chi^2}\right), \tag{3.6}$$

$$\Phi^a_{\chi>1}(\chi) = -\frac{2\Gamma\big(1-\frac{h}{2}\big)\Gamma\big(\frac{h}{2}+\frac{1}{2}\big)}{\sqrt{\pi}}\,\frac{\chi-2}{\chi}\,{}_2F_1\left(\frac{2-h}{2},\frac{h+1}{2},\frac{3}{2},\frac{(\chi-2)^2}{\chi^2}\right). \tag{3.7}$$

These can be extended to the region $0<\chi<1$ by matching their behaviors at $\chi\sim 1$ to appropriate linear combinations of F_1 and F_2. Specifically, as discussed in [6], if $f_{\chi>1}\sim A+B\log(\chi-1)$ as $\chi\to 1^+$, then the corresponding extension $f_{0<\chi<1}$ should approach $A+B\log(1-\chi)$ as $\chi\to 1^-$. In this manner we find that the appropriate expressions in the region $0<\chi<1$ are

$$\Phi^s_{0<\chi<1}(\chi) = AF_1(\chi) + BF_2(\chi)\,, \tag{3.8}$$

$$\Phi^a_{0<\chi<1}(\chi) = BF_1(\chi) + AF_2(\chi)\,, \tag{3.9}$$

where

$$A = \frac{1}{2}\tan(\pi h)\cot\left(\frac{\pi h}{2}\right), \qquad B = -\frac{1}{2}\tan(\pi h)\tan\left(\frac{\pi h}{2}\right). \tag{3.10}$$

Finally, the eigenfunctions can be extended to the region $\chi < 0$ by exploiting the transformation $\chi \to \frac{\chi}{\chi-1}$,

$$\Phi^s_{\chi<0} = +\Phi^s_{0<\chi<1}\left(\frac{\chi}{\chi-1}\right), \qquad \Phi^a_{\chi<0} = -\Phi^a_{0<\chi<1}\left(\frac{\chi}{\chi-1}\right). \tag{3.11}$$

Following [6], the range of allowed values of h can be determined by requiring that the Casimir be hermitian with respect to the inner product

$$\langle g, f\rangle = \frac{1}{2}\int_{-\infty}^{\infty}\frac{d\chi}{\chi^2} g(\chi)^* f(\chi)\,. \tag{3.12}$$

Convergence of this integral requires the eigenfunctions to approach zero at least as fast as $\chi^{1/2}$. This restricts the set of allowed symmetric and antisymmetric eigenfunctions and eigenvalues to

$$\Phi^s_h(\chi) \quad \text{with} \quad h = \frac{1}{2} + is\,,\ s>0\,, \quad \text{or} \quad h = 2n\,,\ n\in\mathbb{Z}_+\,, \tag{3.13}$$

$$\Phi^a_h(\chi) \quad \text{with} \quad h = \frac{1}{2} + is\,,\ s>0\,, \quad \text{or} \quad h = 2n-1\,,\ n\in\mathbb{Z}_+\,. \tag{3.14}$$

Notice that due to the degeneracy under $h \to 1-h$, which originates from the form of the eigenvalue $h(h-1)$ of the Casimir, we can choose to restrict the parameters s in the continuous spectra $h = \frac{1}{2} + is$ to be positive. The continuous series of eigenfunctions admit useful integral representations

$$\Phi^s_h(\chi) = \frac{1}{2}\int_{-\infty}^{\infty}\frac{|\chi|^h}{|y|^h|y-1|^{1-h}|y-\chi|^h}\,dy\,, \tag{3.15}$$

$$\Phi^a_h(\chi) = \frac{\mathrm{sgn}(\chi)}{2}\int_{-\infty}^{\infty}\frac{|\chi|^h\,\mathrm{sgn}(y)\,\mathrm{sgn}(y-1)\,\mathrm{sgn}(y-\chi)}{|y|^h|y-1|^{1-h}|y-\chi|^h}\,dy\,, \tag{3.16}$$

the first of which was pointed out in [6]. These can be explicitly checked by carrying out the integrations in the four different intervals. The continuous eigenfunctions are orthogonal, with

$$\begin{aligned}
\langle \Phi^s_h,\, \Phi^s_{h'}\rangle &= \frac{\pi\tan(\pi h)}{4h-2} 2\pi\delta(h-h')\,,\\
\langle \Phi^a_h,\, \Phi^a_{h'}\rangle &= \frac{\pi\tan(\pi h)}{4h-2} 2\pi\delta(h-h')\,,\\
\langle \Phi^a_h,\, \Phi^s_{h'}\rangle &= 0 = \langle \Phi^s_h,\, \Phi^a_{h'}\rangle\,.
\end{aligned} \tag{3.17}$$

The orthogonality between the symmetric and antisymmetric eigenfunctions can be simply understood as a consequence of the invariance of the measure $d\chi/\chi^2$ under $\chi \to \frac{\chi}{\chi-1}$.

The discrete eigenfunctions can be identified as the real part of the Legendre Q_ν functions of the second kind:

$$\Phi^s_h = 2\,\mathrm{Re}\left(Q_{h-1}\left(\frac{2-\chi}{\chi}\right)\right), \qquad h = 2n\,,\ n\in\mathbb{Z}_+\,, \tag{3.18}$$

$$\Phi^a_h = 2\,\mathrm{Re}\left(Q_{h-1}\left(\frac{2-\chi}{\chi}\right)\right), \qquad h = 2n-1\,,\ n\in\mathbb{Z}_+\,, \tag{3.19}$$

which is a straightforward generalization of [6]. The inner product between the discrete eigenfunctions is simply encapsulated in the formula

$$\langle \Phi_h, \Phi_{h'} \rangle = \frac{\pi^2 \delta_{hh'}}{4h-2} \,. \tag{3.20}$$

In particular, the $\delta_{hh'}$ implies that the symmetric and antisymmetric eigenfunctions are orthogonal since their h parameters must be even and odd, respectively.

We conclude this section by using the completeness relation to write an explicit formula for the eigenfunction decomposition of an arbitrary function $f(\chi)$. Schematically it reads

$$f(\chi) = \sum\!\!\!\!\!\!\int_{h,i} \frac{f^i(h)}{\langle \Phi_h^i, \Phi_h^i \rangle} \Phi_h^i(\chi) \qquad \text{where } f^i(h) \equiv \langle f, \Phi_h^i \rangle \,, \tag{3.21}$$

where the sum over all eigenfunctions includes an index $i \in \{s, a\}$ that accounts for both the symmetric and antisymmetric sectors, and $\sum\!\!\!\!\!\!\int_h$ denotes a sum over the discrete states and an integral over the continuous series. Specifically, using eqs. (3.17) and (3.20), we have

$$f(\chi) = \sum_{h=1}^{\infty} \frac{(4h-2)}{\pi^2} \left\{ \begin{matrix} f^s(h)\Phi_h^s(\chi) \text{ if } h \text{ is even} \\ f^a(h)\Phi_h^a(\chi) \text{ if } h \text{ is odd} \end{matrix} \right\} + \sum_{i \in \{s,a\}} \int_0^{\infty} \frac{ds}{2\pi} \frac{(4h-2)}{\pi \tan(\pi h)} f^i(h) \Phi_h^i(\chi) \,, \tag{3.22}$$

where in the integral it should be understood that $h = \frac{1}{2} + is$. Similarly to the case of [6], this formula can be understood as a single contour integral over a contour in the complex h plane defined as

$$\frac{1}{2\pi i} \int_{\mathcal{C}} dh \equiv \int_{-\infty}^{+\infty} \frac{ds}{2\pi} + \sum_{n=1}^{\infty} \text{Res}_{h=n} \,. \tag{3.23}$$

In this sense, then, we have finally

$$f(\chi) = \frac{1}{2\pi i} \int_{\mathcal{C}} dh \left(\frac{(2h-1) f^s(h)}{\pi \tan\left(\frac{\pi h}{2}\right)} \Phi_h^s(\chi) + \frac{(2h-1) f^a(h)}{\pi \tan\left(\frac{\pi (h-1)}{2}\right)} \Phi_h^a(\chi) \right) . \tag{3.24}$$

4 Evaluating the 4-point functions

Given the complete set of eigenfunctions of the kernels, we are now ready to compute the full 4-point functions in this model, following closely the similar calculation in the fermionic SYK model [4–6]. Throughout this analysis we left out a proper treatment of the (so-called "enhanced") contributions from the lowest $\mathcal{N} = 2$ supermultiplet, although we check at the very end of this section that all divergences in the 4-point functions indeed arise from exchange of this multiplet.

4.1 Setup

There are several independent 4-point functions. We consider first those of the type encountered in section 2.3 for which both pairs of U(N) indices are contracted between fields with the same statistics:

$$\langle \psi_i(\tau_1) \bar{\psi}_i(\tau_2) \psi_j(\tau_3) \bar{\psi}_j(\tau_4) \rangle \,, \quad \langle b_i(\tau_1) \bar{b}_i(\tau_2) \psi_j(\tau_3) \bar{\psi}_j(\tau_4) \rangle \,, \tag{4.1}$$

$$\langle \psi_i(\tau_1) \bar{\psi}_i(\tau_2) b_j(\tau_3) \bar{b}_j(\tau_4) \rangle \,, \quad \langle b_i(\tau_1) \bar{b}_i(\tau_2) b_j(\tau_3) \bar{b}_j(\tau_4) \rangle \,. \tag{4.2}$$

These correlation functions take the form

$$\frac{1}{N^2}\sum_{i,j=1}^{N}\langle\psi_i(\tau_1)\bar{\psi}_i(\tau_2)\psi_j(\tau_3)\bar{\psi}_j(\tau_4)\rangle \tag{4.3}$$

$$= G^{\psi}(\tau_{12})G^{\psi}(\tau_{34}) + \frac{1}{N}\mathcal{F}^{\psi\bar{\psi}\psi\bar{\psi}}(\tau_1,\tau_2,\tau_3,\tau_4) + \mathcal{O}\left(\frac{1}{N^2}\right) \tag{4.4}$$

$$= G^{\psi}(\tau_{12})G^{\psi}(\tau_{34})\left[1 + \frac{1}{N}\mathcal{F}^{\psi\bar{\psi}\psi\bar{\psi}}(\chi) + \mathcal{O}\left(\frac{1}{N^2}\right)\right], \tag{4.5}$$

and similarly for the others. We would like to compute the $\mathcal{F}^{x\bar{x}y\bar{y}}$'s. Notice that we have adopted two conventions for $\mathcal{F}^{x\bar{x}y\bar{y}}$ and it is meant to be understood that when we write the argument as the cross-ratio χ defined in eq. (3.2), we mean the function in (4.5), and when we write the arguments as τ_1, τ_2, τ_3, τ_4, we mean the function in (4.4). The zero-rung (tree-level) contributions to these 4-point functions, which we indicate with a subscript "0", are

$$\mathcal{F}_0^{\psi\bar{\psi}\psi\bar{\psi}}(\tau_1,\tau_2,\tau_3,\tau_4) = G^{\psi}(\tau_{14})G^{\psi}(\tau_{23})\,, \tag{4.6}$$

$$\mathcal{F}_0^{b\bar{b}b\bar{b}}(\tau_1,\tau_2,\tau_3,\tau_4) = G^{b}(\tau_{14})G^{b}(\tau_{23})\,, \tag{4.7}$$

$$\mathcal{F}_0^{\psi\bar{\psi}b\bar{b}}(\tau_1,\tau_2,\tau_3,\tau_4) = \mathcal{F}_0^{b\bar{b}\psi\bar{\psi}}(\tau_1,\tau_2,\tau_3,\tau_4) = 0\,. \tag{4.8}$$

In terms of the cross ratio, the non-zero ones read

$$\mathcal{F}_0^{\psi\bar{\psi}\psi\bar{\psi}}(\chi) = \mathrm{sgn}\left(\frac{\chi}{1-\chi}\right)\left|\frac{\chi}{1-\chi}\right|^{\frac{1}{q}}, \qquad \mathcal{F}_0^{b\bar{b}b\bar{b}}(\chi) = \left|\frac{\chi}{1-\chi}\right|^{\frac{1+q}{q}}. \tag{4.9}$$

Next we decompose the 0-rung correlators (4.9) into the conformal eigenfunctions constructed in the previous section. To this end we first compute the inner products of the 0-rung correlators (4.9) with the symmetric and antisymmetric eigenfunctions, using their integral representations (3.15) and (3.16). These integrals can be evaluated straightforwardly using formula (3.11) of [49] (see also the appendix for more details on these types of integrals), and we find

$$\langle\mathcal{F}_0^{\psi\bar{\psi}\psi\bar{\psi}},\Phi_h^s\rangle = -\frac{\pi\cos^2\left(\frac{\pi}{2q}\right)\Gamma\left(\frac{q-1}{q}\right)^2}{\left(\sin(\pi h)+\sin(\frac{\pi}{q})\right)\Gamma\left(-h-\frac{1}{q}+2\right)\Gamma\left(h-\frac{1}{q}+1\right)} \equiv k_0^{\psi,s}(h)\,, \tag{4.10}$$

$$\langle\mathcal{F}_0^{\psi\bar{\psi}\psi\bar{\psi}},\Phi_h^a\rangle = \frac{\pi\cos^2\left(\frac{\pi}{2q}\right)\Gamma\left(\frac{q-1}{q}\right)^2}{\left(\sin(\frac{\pi}{q})-\sin(\pi h)\right)\Gamma\left(-h-\frac{1}{q}+2\right)\Gamma\left(h-\frac{1}{q}+1\right)} \equiv k_0^{\psi,a}(h)\,, \tag{4.11}$$

$$\langle\mathcal{F}_0^{b\bar{b}b\bar{b}},\Phi_h^s\rangle = \frac{\pi\cos^2\left(\frac{\pi}{2q}\right)\Gamma\left(-\frac{1}{q}\right)^2}{\left(\sin(\pi h)+\sin(\frac{\pi}{q})\right)\Gamma\left(-h-\frac{1}{q}+1\right)\Gamma\left(h-\frac{1}{q}\right)} \equiv k_0^{b,s}(h)\,, \tag{4.12}$$

$$\langle\mathcal{F}_0^{b\bar{b}b\bar{b}},\Phi_h^a\rangle = \frac{\pi\cos^2\left(\frac{\pi}{2q}\right)\Gamma\left(-\frac{1}{q}\right)^2}{\left(\sin(\pi h)-\sin(\frac{\pi}{q})\right)\Gamma\left(-h-\frac{1}{q}+1\right)\Gamma\left(h-\frac{1}{q}\right)} \equiv k_0^{b,a}(h)\,. \tag{4.13}$$

The two 4-point functions in eq. (4.1) are closed under iterating the kernel shown in figure 2, as are the two shown in eq. (4.2). We consider the two pairs in turn, since the calculations are essentially identical.

JHEP10(2017)202

4.2 The $\psi\bar{\psi}\psi\bar{\psi}$ and $b\bar{b}\psi\bar{\psi}$ 4-point functions

The eigenfunction expansion of $\mathcal{F}_0^{\psi\bar{\psi}\psi\bar{\psi}}(\chi)$ is given by plugging $k_0^{\psi,s}(h)$ and $k_0^{\psi,a}(h)$ into the completeness relation (3.24). We can write this as

$$\mathcal{F}_0^{\psi\bar{\psi}\psi\bar{\psi}}(\chi) = \frac{1}{2\pi i}\int_{\mathcal{C}} dh\big(f_0^s(h) + f_0^a(h)\big) \tag{4.14}$$

where

$$f_0^s(h) = \frac{(2h-1)k_0^{\psi,s}(h)}{\pi\tan\left(\frac{\pi h}{2}\right)}\Phi_h^s(\chi)\,, \qquad f_0^a(h) = \frac{(2h-1)k_0^{\psi,a}(h)}{\pi\tan\left(\frac{\pi(h-1)}{2}\right)}\Phi_h^a(\chi)\,. \tag{4.15}$$

Although $\mathcal{F}_0^{b\bar{b}\psi\bar{\psi}}(\chi) = 0$, let us still write it as

$$\mathcal{F}_0^{b\bar{b}\psi\bar{\psi}}(\chi) = \frac{1}{2\pi i}\int_{\mathcal{C}} dh\big(m_0^s(h) + m_0^a(h)\big)\,, \qquad m_0^{s,a}(h) = 0\,, \tag{4.16}$$

so that it serves as a starting point of the repeated action by the kernel matrix.

Starting from the zero-rung ladders characterized by $f_0^{s,a}(h)$ and $m_0^{s,a}(h)$, we generate the n-rung ladder contribution to the 4-point functions by convolving n times with the kernel matrix (2.25). The full 4-point functions are then determined by the geometric series

$$f^{s,a}(h) = \sum_{n=0}^{\infty} f_n^{s,a}(h)\,, \qquad m^{s,a}(h) = \sum_{n=0}^{\infty} m_n^{s,a}(h)\,. \tag{4.17}$$

From our previous analysis and the integral relations

$$\frac{\mathrm{sgn}(\tau_{12})\,\mathrm{sgn}(\tau_{34})}{|\tau_{12}|^{2\Delta}|\tau_{34}|^{2\Delta}}\Phi_h^s = +\frac{1}{2}\int d\tau_0 \frac{\mathrm{sgn}(\tau_{12})}{|\tau_{10}|^h|\tau_{20}|^h|\tau_{12}|^{2\Delta-h}}\frac{\mathrm{sgn}(\tau_{34})}{|\tau_{30}|^{1-h}|\tau_{40}|^{1-h}|\tau_{34}|^{2\Delta-1+h}}\,, \tag{4.18}$$

$$\frac{\mathrm{sgn}(\tau_{12})\,\mathrm{sgn}(\tau_{34})}{|\tau_{12}|^{2\Delta}|\tau_{34}|^{2\Delta}}\Phi_h^a = -\frac{1}{2}\int d\tau_0 \frac{\mathrm{sgn}(\tau_{01})\,\mathrm{sgn}(\tau_{02})}{|\tau_{10}|^h|\tau_{20}|^h|\tau_{12}|^{2\Delta-h}}\frac{\mathrm{sgn}(\tau_{03})\,\mathrm{sgn}(\tau_{04})}{|\tau_{30}|^{1-h}|\tau_{40}|^{1-h}|\tau_{34}|^{2\Delta-1+h}}\,, \tag{4.19}$$

we conclude that (f_n^s, m_n^s) close under the action of the kernels K_c^{11}, K_c^{12}, K_c^{21} with eigenvalues $k_c^{a,11}$, $k_c^{a,12}$, $k_c^{a,21}$ respectively; while (f_n^a, m_n^a) is another basis on which the kernels K^{11}, K^{12}, K^{21} have eigenvalues $k_c^{s,11}$, $k_c^{s,12}$, $k_c^{s,21}$ respectively.

Let us consider the symmetric sector first; the action of the kernel matrix on an n-rung ladder is

$$\begin{pmatrix} f_{n+1}^s \\ m_{n+1}^s \end{pmatrix} = \begin{pmatrix} k_c^{a,11} & k_c^{a,12} \\ k_c^{a,21} & 0 \end{pmatrix}\begin{pmatrix} f_n^s \\ m_n^s \end{pmatrix}. \tag{4.20}$$

We can diagonalize the matrix as

$$\begin{pmatrix} f_{n+1}^s \\ m_{n+1}^s \end{pmatrix} = U^{a\dagger}\begin{pmatrix} \widetilde{k}_c^{a,-} & (k_c^{a,21} - k_c^{a,12})\,\mathrm{sgn}(k_c^{a,21}) \\ 0 & \widetilde{k}_c^{a,+} \end{pmatrix} U^a \begin{pmatrix} f_n^s \\ m_n^s \end{pmatrix}, \tag{4.21}$$

where the $\widetilde{k}$'s are defined in footnote 1, and the transformation matrix is $U^a = U(k_c^{a,11}, k_c^{a,12}, k_c^{a,21})$ with

$$U(x,y,z) = \frac{1}{\sqrt{-x\sqrt{x^2+4yz}+x^2+2yz+2z^2}}\begin{pmatrix} -\frac{\sqrt{x^2+4yz}-x}{\sqrt{2}\,\mathrm{sgn}(z)} & \sqrt{2}|z| \\ \sqrt{2}z & \frac{\sqrt{x^2+4yz}-x}{\sqrt{2}} \end{pmatrix}. \tag{4.22}$$

The contribution from the n-rung ladder diagram can then be solved straightforwardly:

$$\begin{pmatrix} f_n^s \\ m_n^s \end{pmatrix} = U^{a,\dagger} \begin{pmatrix} (\widetilde{k}_c^{a,-})^n & (k_c^{a,21} - k_c^{a,12}) \frac{(\widetilde{k}_c^{a,-})^n - (\widetilde{k}_c^{a,+})^n}{\widetilde{k}_c^{a,-} - \widetilde{k}_c^{a,+}} \operatorname{sgn}(k_c^{a,21}) \\ 0 & (\widetilde{k}_c^{a,+})^n \end{pmatrix} U^a \begin{pmatrix} f_0^s \\ m_0^s \end{pmatrix}. \tag{4.23}$$

Summing over all such diagrams as in eq. (4.17) then gives

$$\begin{pmatrix} f^s \\ m^s \end{pmatrix} = U^{a,\dagger} \begin{pmatrix} \frac{1}{1-\tilde{k}_c^{a,-}} & \frac{k_c^{a,21} - k_c^{a,12}}{(1-\tilde{k}_c^{a,-})(1-\tilde{k}_c^{a,+})} \operatorname{sgn}(k_c^{a,21}) \\ 0 & \frac{1}{1-\tilde{k}_c^{a,+}} \end{pmatrix} U^a \begin{pmatrix} f_0^s \\ m_0^s \end{pmatrix}. \tag{4.24}$$

Multiplying through by the U matrices leads to,

$$\begin{pmatrix} f^s \\ m^s \end{pmatrix} = \frac{1}{(1-\tilde{k}_c^{a,-})(1-\tilde{k}_c^{a,+})} \begin{pmatrix} 1 & k_c^{a,12} \\ k_c^{a,21} & 1 - k_c^{a,11} \end{pmatrix} \begin{pmatrix} f_0^s \\ m_0^s \end{pmatrix}. \tag{4.25}$$

Finally, since $m_0^s = 0$, we have simply

$$f^s(h) = \frac{f_0^s(h)}{(1-\widetilde{k}_c^{a,-})(1-\widetilde{k}_c^{a,+})}, \qquad m^s(h) = \frac{k_c^{a,21} f_0^s(h)}{(1-\widetilde{k}_c^{a,-})(1-\widetilde{k}_c^{a,+})}. \tag{4.26}$$

The calculation in the antisymmetric sector proceeds in the same way, leading to exactly the same result but with the "s" and "a" superscripts exchanged.

The full 4-point functions are then given by

$$\mathcal{F}^{\psi\bar{\psi}\psi\bar{\psi}}(\chi) = \frac{1}{2\pi i} \int_{\mathcal{C}} dh \big(f^s(h) + f^a(h)\big), \qquad \mathcal{F}^{b\bar{b}\psi\bar{\psi}}(\chi) = \frac{1}{2\pi i} \int_{\mathcal{C}} dh \big(m^s(h) + m^a(h)\big). \tag{4.27}$$

As in the pure fermionic case (see [6] for details), we can move the contour in the positive real direction to pick up only the contributions from the poles at $\widetilde{k}_c^{i,+} = 1$ — the factors $1 - \widetilde{k}_c^{i,-}$ in the denominator never vanish since $\widetilde{k}_c^{i,-}$ is always negative, and the poles of the $k_c^{i,21}$ factors in the numerator are all cancelled by poles in the denominator. In the $\chi > 1$ region this contour deformation is straightforward and leads to

$$\mathcal{F}^{\psi\bar{\psi}\psi\bar{\psi}}(\chi) = -\sum_{i\in\{s,a\}} \sum_m \operatorname*{Res}_{h=\widetilde{h}_m^{i,+}} \left(\frac{f_0^{\bar{i}}(h)}{(1-\widetilde{k}_c^{i,-})(1-\widetilde{k}_c^{i,+})} \right), \qquad \chi > 1, \tag{4.28}$$

$$\mathcal{F}^{b\bar{b}\psi\bar{\psi}}(\chi) = -\sum_{i\in\{s,a\}} \sum_m \operatorname*{Res}_{h=\widetilde{h}_m^{i,+}} \left(\frac{k_c^{i,21} f_0^{\bar{i}}(h)}{(1-\widetilde{k}_c^{i,-})(1-\widetilde{k}_c^{i,+})} \right), \qquad \chi > 1, \tag{4.29}$$

where the sums run over the roots of $1 - \widetilde{k}_c^{i,+}(h) = 0$, enumerated here as $\widetilde{h}_m^{i,+}$, and $\bar{i}$ means the complement of i in the set $\{s, a\}$. In the $\chi < 1$ region, we meet a similar problem of negative entries of the hypergeometric function as that encountered in [6]. It is straightforward to generalize their treatment to our case; the net effect is to replace the $\Phi_h^{a,s}$ by $\frac{\chi^h \Gamma(h)^2}{\Gamma(2h)} {}_2F_1(h,h;2h;\chi)$. Therefore, the formulas (4.28) and (4.29) can be extended to the region $0 < \chi < 1$ by replacing the $f_0^i(h)$'s with

$$\widetilde{f}_0^s(h) = \frac{(2h-1)k_0^{\psi,s}(h)}{\pi \tan\left(\frac{\pi h}{2}\right)} \frac{\chi^h \Gamma(h)^2}{\Gamma(2h)} {}_2F_1(h,h;2h;\chi), \tag{4.30}$$

$$\widetilde{f}_0^a(h) = \frac{(2h-1)k_0^{\psi,a}(h)}{\pi \tan\left(\frac{\pi(h-1)}{2}\right)} \frac{\chi^h \Gamma(h)^2}{\Gamma(2h)} {}_2F_1(h,h;2h;\chi). \tag{4.31}$$

4.3 The $\psi\bar{\psi}b\bar{b}$ and $b\bar{b}b\bar{b}$ 4-point functions

The other two 4-point functions can be computed similarly. We begin with the eigenfunction decompositions of the 0-rung ladders

$$\mathcal{F}_0^{b\bar{b}b\bar{b}}(\chi) = \frac{1}{2\pi i}\int_{\mathcal{C}} dh \big(b_0^s(h) + b_0^a(h)\big)\,, \tag{4.32}$$

$$\mathcal{F}_0^{\psi\bar{\psi}b\bar{b}}(\chi) = \frac{1}{2\pi i}\int_{\mathcal{C}} dh \big(p_0^s(h) + p_0^a(h)\big)\,, \tag{4.33}$$

with

$$b_0^s(h) = \frac{(2h-1)k_0^{b,s}}{\pi\tan\left(\frac{\pi h}{2}\right)}\Phi_h^s(\chi)\,, \qquad b_0^a(h) = \frac{(2h-1)k_0^{b,a}}{\pi\tan\left(\frac{\pi(h-1)}{2}\right)}\Phi_h^a(\chi)\,, \qquad p_0^{s,a}(h) = 0\,. \tag{4.34}$$

The calculation proceeds the same as in the previous subsection, except with $(f,m)\mapsto(p,b)$, all the way through eq. (4.25). At that step we plug in eq. (4.34) which leads to

$$p^s(h) = \frac{k_c^{a,12}b_0^s(h)}{(1-\widetilde{k}_c^{a,-})(1-\widetilde{k}_c^{a,+})}\,, \qquad b^s(h) = \frac{(1-k_c^{a,11})b_0^s(h)}{(1-\widetilde{k}_c^{a,-})(1-\widetilde{k}_c^{a,+})}\,, \tag{4.35}$$

again together with the same equation but with the "s" and "a" superscripts exchanged.

With these results, the full 4-point functions are then

$$\mathcal{F}^{\psi\bar{\psi}b\bar{b}}(\chi) = -\sum_{i\in\{s,a\}}\sum_m \operatorname*{Res}_{h=\widetilde{h}_m^{i,+}}\left(\frac{k_c^{i,12}b_0^{\bar{i}}(h)}{(1-\widetilde{k}_c^{i,-})(1-\widetilde{k}_c^{i,+})}\right), \qquad \chi>1\,, \tag{4.36}$$

$$\mathcal{F}^{b\bar{b}b\bar{b}}(\chi) = -\sum_{i\in\{s,a\}}\sum_m \operatorname*{Res}_{h=\widetilde{h}_m^{i,+}}\left(\frac{(1-k_c^{i,11})b_0^{\bar{i}}(h)}{(1-\widetilde{k}_c^{i,-})(1-\widetilde{k}_c^{i,+})}\right), \qquad \chi>1\,. \tag{4.37}$$

As we saw in the previous subsection, these formulas can be extended to the region $0<\chi<1$ by replacing the $b_0^i(h)$'s with

$$\widetilde{b}_0^s(h) = \frac{(2h-1)k_0^{b,s}(h)}{\pi\tan\left(\frac{\pi h}{2}\right)}\frac{\chi^h\Gamma(h)^2}{\Gamma(2h)}\,{}_2F_1(h,h;2h;\chi)\,, \tag{4.38}$$

$$\widetilde{b}_0^a(h) = \frac{(2h-1)k_0^{b,a}(h)}{\pi\tan\left(\frac{\pi(h-1)}{2}\right)}\frac{\chi^h\Gamma(h)^2}{\Gamma(2h)}\,{}_2F_1(h,h;2h;\chi)\,. \tag{4.39}$$

4.4 The $\psi b\bar{\psi}\bar{b}$ 4-point function

Finally we turn to the $\langle\psi_i(\tau_1)b_i(\tau_2)\bar{\psi}_j(\tau_3)\bar{b}_j(\tau_4)\rangle$ 4-point function, which is more subtle. It has no disconnected contributions, taking the form

$$\frac{1}{N^2}\sum_{i,j=1}^N\langle\psi_i(\tau_1)b_i(\tau_2)\bar{\psi}_j(\tau_3)\bar{b}_j(\tau_4)\rangle = \frac{1}{N}\mathcal{F}^{\psi b\bar{\psi}\bar{b}}(\tau_1,\tau_2,\tau_3,\tau_4) + \mathcal{O}\left(\frac{1}{N^2}\right), \tag{4.40}$$

with the 0-rung correlator being simply

$$\mathcal{F}_0^{\psi b\bar{\psi}\bar{b}}(\tau_1,\tau_2,\tau_3,\tau_4) = G^{\psi}(\tau_{13})G^b(\tau_{24}) = \frac{1}{q}\left(\frac{\tan\left(\frac{\pi}{2q}\right)}{2\pi J}\right)^{2/q}\frac{\mathrm{sgn}(\tau_{13})}{|\tau_{13}|^{\frac{1}{q}}}\frac{1}{|\tau_{24}|^{\frac{1+q}{q}}}\,. \tag{4.41}$$

We would like to continue working with the conformal eigenfunctions from section 3. In order to do this we would have to factor out some appropriate overall τ dependence in order to render eq. (4.41) a function of the cross-ratio χ, as for example between eqs. (4.4) and (4.5). We can't, however, divide by the obvious candidate $G^{\psi}(\tau_{13})G^{b}(\tau_{24})$ as this would give us $\mathcal{F}_0(\chi) = 1$, and the function "1" is not in the allowed spectrum; it would correspond to the discrete state $h = 0$ in eq. (3.13), which is absent because it is not normalizable with respect to (3.12).

Let us instead notice that the tree-level 4-point function can be expressed as

$$\mathcal{F}_0^{\psi b\bar{\psi}\bar{b}}(\tau_1,\tau_2,\tau_3,\tau_4) = \partial_{\tau_4}\mathcal{G}_0(\tau_1,\tau_2,\tau_3,\tau_4) \tag{4.42}$$

in terms of the auxiliary quantity

$$\mathcal{G}_0(\tau_1,\tau_2,\tau_3,\tau_4) = \left(\frac{\tan\left(\frac{\pi}{2q}\right)}{2\pi J}\right)^{2/q} \frac{\operatorname{sgn}(\tau_{13})\operatorname{sgn}(\tau_{24})}{|\tau_{13}|^{\frac{1}{q}}|\tau_{24}|^{\frac{1}{q}}}\,. \tag{4.43}$$

This derivative might introduce a spurious $\delta(\tau_{24})$ contact term, but since we are not interested in any such terms we can in practice just commit ourselves to neglecting all possible contact terms at the very end of any calculation. It is evident from the powers of the denominator factors in eq. (4.43) that we should think of $\mathcal{G}$ roughly as a four-fermion correlator; this will tell us, in particular, the conformal of the eigenfunctions we should use when diagonalizing the relevant kernel.

Now consider the action of some kernel K on $\mathcal{G}_0$, defined by

$$\mathcal{G}_1(\tau_1,\tau_2,\tau_3,\tau_4) = \int d\tau_5 d\tau_6 K(\tau_1,\tau_2;\tau_5,\tau_6)\mathcal{G}_0(\tau_5,\tau_6,\tau_3,\tau_4)\,. \tag{4.44}$$

It is evident that taking a τ_4 derivative commutes with the action of the ladder kernel, and this property clearly extends to arbitrary order as we iterate the kernel. Therefore, the full 4-point function $\mathcal{F}^{\psi b\bar{\psi}\bar{b}}$ can be obtained by first computing the sum of all ladder contributions to $\mathcal{G}$ using the kernel (2.13) and then taking ∂_{τ_4}. To compute the latter we begin by constructing an appropriate function of the cross-ratio χ by factoring out the same prefactor as in the four-fermion function (4.5), defining

$$\mathcal{G}_0(\chi) \equiv \frac{\mathcal{G}_0(\tau_1,\tau_2,\tau_3,\tau_4)}{G^{\psi}(\tau_{12})G^{\psi}(\tau_{34})} = \operatorname{sgn}(\chi)|\chi|^{\frac{1}{q}}\,. \tag{4.45}$$

Now we can decompose $\mathcal{G}_0(\chi)$ into the conformal eigenfunctions by plugging its matrix elements

$$\langle \mathcal{G}_0, \Phi_h^s\rangle = \frac{\pi\cos^2\left(\frac{\pi}{2q}\right)\Gamma\left(\frac{q-1}{q}\right)^2}{\left(\sin(\pi h)+\sin(\frac{\pi}{q})\right)\Gamma\left(-h-\frac{1}{q}+2\right)\Gamma\left(h-\frac{1}{q}+1\right)} = k_0^s(h)\,, \tag{4.46}$$

$$\langle \mathcal{G}_0, \Phi_h^a\rangle = \frac{\pi\cos^2\left(\frac{\pi}{2q}\right)\Gamma\left(\frac{q-1}{q}\right)^2}{\left(\sin(\frac{\pi}{q})-\sin(\pi h)\right)\Gamma\left(-h-\frac{1}{q}+2\right)\Gamma\left(h-\frac{1}{q}+1\right)} = k_0^a(h) \tag{4.47}$$

into the completness relation (3.24).

Since the relevant kernel K_c^d is diagonal, much of the complication encountered in the previous two subsections is avoided. The sum over ladder diagrams just inserts a geometric series factor $1/\big(1-k^i(h)\big)$ into the conformal eigenfunction decomposition, where $k^i(h)$ are the eigenvalues of the kernel. However, we should not use the formulas (2.20) and (2.21) since those are the eigenvalues of K_c^d when acting on eigenfunctions of the form (2.16) and (2.17). Since we are iterating the action of K_c^d on $\mathcal{G}$, which should be treated like a four-fermion correlator, we must work out the eigenvalues of K_c^d when acting on eigenfunctions of the form (2.16) and (2.17) with $2\Delta_\psi$ replacing $\Delta_\psi+\Delta_b$. This is readily accomplished by substituting $h\to h+\frac{1}{2}$ in eqs. (2.16) and (2.17), and hence also into eqs. (2.20) and (2.21). The resulting symmetric and antisymmetric eigenvalues can be expressed in terms of the matrix elements of $\mathcal{G}_0$ as

$$\begin{aligned} k_c^{o,s}(h) &= k_c^{s,d}\left(h+\frac{1}{2}\right) = 4\alpha q\left(h-1+\frac{1}{q}\right)k_0^a(h)\,,\\ k_c^{o,a}(h) &= k_c^{a,d}\left(h+\frac{1}{2}\right) = 4\alpha q\left(h-1+\frac{1}{q}\right)k_0^s(h)\,. \end{aligned} \tag{4.48}$$

Before proceeding, however, we should make here one comment about the operator spectrum in this channel. The dimensions of the operators running in this channel are encoded in the divergences of the 4-point function, which occur at the values of h such that

$$k_c^{o,i}(h)=1\,,\qquad i\in\{s,a\}\,. \tag{4.49}$$

However, this h itself does not directly correspond to the operators in the original 4-point function $\mathcal{F}^{\psi b\psi b}$. To see this, let us recall that as noted by [5, 6, 50], the eigenfunctions are naturally dressed with additional factors that allow them to be expressed as 3-point functions whose form is dictated by conformal symmetry. We have used this implicitly in previous sections but here we must be more explicit, writing the eigenfunction for example as eq. (3.69) of [6]:

$$\frac{\mathrm{sgn}(\tau_{12})}{|\tau_{10}|^{h_o-1/2}|\tau_{20}|^{h_o+1/2}|\tau_{12}|^{\Delta_\psi+\Delta_b-h_o}}\,, \tag{4.50}$$

where h^o is the dimension of the 3rd operator propagating in the channel.

But, as we have already mentioned, in the present computation, the appropriate eigenfunctions are not eq. (4.50) but rather

$$\frac{\mathrm{sgn}(\tau_{12})}{|\tau_{10}|^{h}|\tau_{20}|^{h}|\tau_{12}|^{2\Delta_\psi-h}}\,. \tag{4.51}$$

Comparing the two expressions, in particular the power of the last term,[2] which is the one that enters directly into the integrals that compute the eigenvalues (cf. eqs. (2.16)

[2]The seeming mismatch of the power of $|\tau_{20}|$ does not matter since we can always move τ_0 to infinity using conformal invariance, without affecting the result of the calculation. Another way to understand this is to notice that the power of τ_2 will be corrected once we take the τ_4 derivative; this will produce an extra power of $1/\tau_{24}$ in the end.

JHEP10(2017)202

and (2.17)), we see that the real dimension h^o of the operator running in the original 4-point function $\mathcal{F}^{\psi b\bar{\psi}\bar{b}}$ is related to h by

$$h = h_o - \frac{1}{2}\,. \tag{4.52}$$

Indeed, as a check of this relation, we see that the solution to (4.49), together with the shift (4.52), does give the correct dimensions (2.20), (2.21) (as manifested already in (4.48)).

With this important comment out of the way, we are ready to write the sum over all ladder diagrams

$$\mathcal{G}(\chi) = \sum_{i\in\{s,a\}} \frac{1}{2\pi i}\int_{\mathcal{C}} dh \frac{g^{\bar{i}}(h)}{1-k_c^{o,i}(h)}\Phi_h^{\bar{i}}\,, \tag{4.53}$$

where

$$g^s(h) = \frac{(2h-1)k_0^s}{\pi\tan\left(\frac{\pi h}{2}\right)}\,, \qquad g^a(h) = \frac{(2h-1)k_0^a}{\pi\tan\left(\frac{\pi(h-1)}{2}\right)}\,. \tag{4.54}$$

Notice however that $h=1$ is a solution to both $k_c^{o,a}(h)=1$ and $k_c^{o,s}(h)=1$, therefore in the discrete sum of the odd series Φ_h^a, the $h=1$ term diverges. This corresponds to an enhancement due to a mode of dimension $h_o=\frac{3}{2}$ that is is similar to the $h=2$ enhancement appearing in the fermionic SYK model [6, 84]. In the following computation, we have excluded such enhanced contributions.

We can then push the contour to the right, picking up contributions from poles of the factor $\frac{k_0^{\bar{i}}}{1-k_c^{o,i}(h)}$. Due to the proportionality (4.48) between $k_0^{\bar{i}}$ and $k_c^{o,i}$, the poles of the numerator $k_0^{\bar{i}}$ are cancelled by poles of $k_c^{o,i}$ in the denominator and thus the only contribution comes from solutions to $k_c^{o,i}(h)=1$. Furthermore, in light of eq. (4.48), these poles correspond to the set $h_m^{\bar{i},d}-\frac{1}{2}$, where $h_m^{\bar{i},d}$ are the solutions to $k_c^{\bar{i},d}(h)=1$, i.e. the dimensions of states propagating in the OPE channel of the diagonal kernel. For the $\chi>1$ region, this contour manipulation is straightforward and leads to

$$\mathcal{G}(\chi) = -\sum_{i\in\{s,a\}}\sum_m \operatorname*{Res}_{h=h_m^{\bar{i},d}-\frac{1}{2}}\left(\frac{g^{\bar{i}}(h)}{1-k_c^{o,i}(h)}\Phi_h^{\bar{i}}\right), \qquad \chi>1\,. \tag{4.55}$$

As in the previous subsections, we replace the $\Phi_h^{a,s}$ by $\frac{\chi^h\Gamma(h)^2}{\Gamma(2h)}\,{}_2F_1(h,h;2h;\chi)$ to obtain

$$\mathcal{G}(\chi) = -\sum_{i\in\{s,a\}}\sum_m \operatorname*{Res}_{h=h_m^{\bar{i},d}-\frac{1}{2}}\left(\frac{g^{\bar{i}}(h)}{1-k_c^{o,i}(h)}\frac{\chi^h\Gamma(h)^2}{\Gamma(2h)}\,{}_2F_1(h,h;2h;\chi)\right), \qquad 0<\chi<1\,.$$

This concludes our calculation of the auxiliary quantity $\mathcal{G}$, but it remains to compute the original 4-point function

$$\mathcal{F}^{\psi b\bar{\psi}\bar{b}}(\tau_1,\tau_2,\tau_3,\tau_4) = \partial_{\tau_4}\mathcal{G}(\tau_1,\tau_2,\tau_3,\tau_4)\,. \tag{4.56}$$

This τ_4 derivative can be worked out explicitly. Making use of a property of the hypergeometric function and

$$\partial_{\tau_4}\chi = -\frac{\tau_{12}\tau_{23}}{\tau_{13}\tau_{24}^2} = -\chi\frac{\tau_{23}}{\tau_{34}\tau_{24}}\,, \tag{4.57}$$

the derivative is equivalent to replacing the ${}_2F_1(h,h;2h;\chi)$ by the factor

$$\frac{\text{sgn}(\tau_{34})}{|\tau_{34}|}\left(\frac{1}{q}\,{}_2F_1(h,h;2h;\chi)-\frac{\tau_{23}}{\tau_{24}}h\,{}_2F_1(h,h+1;2h;\chi)\right). \tag{4.58}$$

The replacement for ${}_2F_1(1-h,1-h;2-2h;\chi)$ can be obtained from (4.58) by sending $h\to 1-h$.

Notice that the computation in this subsection is secretly making use of the supersymmetry Ward identity. The supersymmetry transformation on the bosonic fields take the schematic form $Qb\to\partial\psi$. Therefore, the step of taking a derivative in our computation, which we saw essentially converts a fermionic factor into a bosonic one, is essentially using supersymmetry to relate the computation in this subsection to a similar computation in section 4.2. In fact, the result (4.56) has a form that manifestly satisfies a supersymmetry Ward identity.

Furthermore, we note from the expressions (4.26) and (4.35), that the $\Phi_2^s(\chi)$ term becomes divergent at $h=2=h_0^{a,-}$ and the $\Phi_1^a(\chi)$ term becomes divergent at $h=1=h_0^{s,+}$. From the expression (4.53), the $\Phi_1^a(\chi)$ term becomes divergent at $h=1=h^{o,a,+}=h_0^{s,d}$. This confirms that all divergences arise from contributions from the first $\mathcal{N}=2$ supermultiplet $(h_0^{s,+},h_0^{s,d},h_0^{a,-})$. This agrees with the expectation of [84]. The proper treatment of these divergences leads to enhanced contributions to the 4-point functions along the lines of the analysis for the fermionic SYK model, i.e. section 3.3 of [6]. Schematically, the required computation includes perturbing away from the conformal limit, getting the corrections to the propagators, deriving the corrections to the eigenvalues corresponding to the $h=2$ supermultiplet, and finally obtaining the regularized contribution to the 4-point function. This computation has not yet been repeated even for the simpler $\mathcal{N}=1$ supersymmetric model and is beyond the scope of this paper. We hope to carry it out elsewhere.

5 6-point functions

A natural next step would be to compute 6-point correlation functions to extract the OPE coefficients among the singlet bilinear operators of the model. This would be a supersymmetric generalization of the work [32], and we will follow many of the notations employed there. Given all the 4-point functions that we have worked out, we can take their OPE limits and read out the structure constants c_n^{xy} according to

$$\frac{1}{N}\sum_{i=1}^{N}x_i(\tau_1)y_i(\tau_2)=\text{sgn}(\tau_{12})^{d(x)d(y)}\frac{|\tau_{12}|^{h_n-h_x-h_y}}{\sqrt{N}}\sum_n c_n^{xy}\,F_{\mathcal{O}_n}(\tau_2)\,, \tag{5.1}$$

where $x,y\in\{\psi,b\}$, $d(\psi)=1$, $d(b)=0$, and

$$F_{\mathcal{O}_n}(\tau)=\left(1+\frac{1}{2}\tau\partial_\tau+\cdots\right)\mathcal{O}_n(\tau) \tag{5.2}$$

is a family of operators containing the primary $\mathcal{O}_n$ and all of its descendents. In practice, the coefficients c_n^{xy} can be read off from a 4-point function by restoring all of the time

dependence via (3.2) and expanding it into the form

$$\mathcal{F}^{xyzw}(\tau_1,\tau_2,\tau_3,\tau_4)=\frac{\mathrm{sgn}(\tau_{12})^{d(x)d(y)}}{|\tau_{12}|^{h_1+h_2}}\frac{\mathrm{sgn}(\tau_{34})^{d(z)d(w)}}{|\tau_{34}|^{h_3+h_4}}\sum_n\frac{|c_n^{\phi\phi}|^2}{|\tau_{12}|^{-h_n}|\tau_{34}|^{-h_n}|\tau_{24}|^{2h_n}} \tag{5.3}$$

in the OPE limit

$$|\tau_{12}|\ll|\tau_{24}|\,,\qquad |\tau_{34}|\ll|\tau_{24}|\,. \tag{5.4}$$

With these coefficients extracted out, one can easily check that there are again two different types of contributing diagrams to the leading order in the large-N limit of the supersymmetric SYK model. Because we are treating the supersymmetric model in component form, the computations are almost the same as those in section 3 of [32]. In particular, we would need to compute exactly the same integrals $I^{(1)}_{mnp}$ and $I^{(2)}_{mnp}$. The only difference is that we have more possible external configurations and thus would need to sum over more combinations of $c_n^{\phi\phi}$. Since the computation will be largely identical to those in [32], we will not elaborate any details here.

Acknowledgments

We thank Micha Berkooz, Antal Jevicki and Moshe Rozali for useful discussions on related topics. This work was supported by the U.S. Department of Energy under contract DE-SC0010010 Task A and by Simons Investigator Award #376208 (AV). CP thanks the Galileo Galilei Institute for Theoretical Physics (GGI) for hospitality within the program "New Developments in AdS3/CFT2 Holography", during which period he was partially supported by a Young Investigator Training Program fellowship from INFN as well as the ACRI (Associazione di Fondazioni e di Casse di Risparmio S.p.a.).

A Useful integrals

Here we tabulate some useful integrals:

$$\int dt\,dt'\frac{\mathrm{sgn}(t_1-t)\,\mathrm{sgn}(t_2-t')\,\mathrm{sgn}(t-t')}{|t_1-t|^{2\alpha}|t_2-t'|^{2\beta}|t-t'|^{2\gamma}}= \frac{\pi^2\sin\big(\pi(\alpha+\beta+\gamma-1)\big)\Gamma(2\alpha+2\beta+2\gamma-2)}{\sin(\pi\alpha)\Gamma(2\alpha)\sin(\pi\beta)\Gamma(2\beta)\sin(\pi\gamma)\Gamma(2\gamma)}\frac{\mathrm{sgn}(t_{12})}{|t_{12}|^{2\alpha+2\beta+2\gamma-2}}\,, \tag{A.1}$$

$$\int dt\,dt'\frac{\mathrm{sgn}(t_1-t)\,\mathrm{sgn}(t_2-t')}{|t_1-t|^{2\alpha}|t_2-t'|^{2\beta}|t-t'|^{2\gamma}}= \frac{\pi^2\cos\big(\pi(\alpha+\beta+\gamma-1)\big)\Gamma(2\alpha+2\beta+2\gamma-2)}{\sin(\pi\alpha)\Gamma(2\alpha)\sin(\pi\beta)\Gamma(2\beta)\cos(\pi\gamma)\Gamma(2\gamma)}\frac{1}{|t_{12}|^{2\alpha+2\beta+2\gamma-2}}\,, \tag{A.2}$$

$$\int dt\,dt'\frac{\mathrm{sgn}(t_1-t)\,\mathrm{sgn}(t-t')}{|t_1-t|^{2\alpha}|t_2-t'|^{2\beta}|t-t'|^{2\gamma}}= -\frac{\pi^2\cos\big(\pi(\alpha+\beta+\gamma-1)\big)\Gamma(2\alpha+2\beta+2\gamma-2)}{\sin(\pi\alpha)\Gamma(2\alpha)\cos(\pi\beta)\Gamma(2\beta)\sin(\pi\gamma)\Gamma(2\gamma)}\frac{1}{|t_{12}|^{2\alpha+2\beta+2\gamma-2}}\,, \tag{A.3}$$

$$\int dt\, dt' \frac{\mathrm{sgn}(t_1-t)}{|t_1-t|^{2\alpha}|t_2-t'|^{2\beta}|t-t'|^{2\gamma}} = \frac{\pi^2 \sin\big(\pi(\alpha+\beta+\gamma-1)\big)\Gamma(2\alpha+2\beta+2\gamma-2)}{\sin(\pi\alpha)\Gamma(2\alpha)\cos(\pi\beta)\Gamma(2\beta)\cos(\pi\gamma)\Gamma(2\gamma)} \frac{\mathrm{sgn}(t_{12})}{|t_{12}|^{2\alpha+2\beta+2\gamma-2}}\,. \tag{A.4}$$

$$\int dt\, dt' \frac{\mathrm{sgn}(t-t')}{|t_1-t|^{2\alpha}|t_2-t'|^{2\beta}|t-t'|^{2\gamma}} = \frac{\pi^2 \sin\big(\pi(\alpha+\beta+\gamma-1)\big)\Gamma(2\alpha+2\beta+2\gamma-2)}{\cos(\pi\alpha)\Gamma(2\alpha)\cos(\pi\beta)\Gamma(2\beta)\sin(\pi\gamma)\Gamma(2\gamma)} \frac{\mathrm{sgn}(t_{12})}{|t_{12}|^{2\alpha+2\beta+2\gamma-2}}\,, \tag{A.5}$$

and

$$\int dt\, dt' \frac{1}{|t_1-t|^{2\alpha}|t_2-t'|^{2\beta}|t-t'|^{2\gamma}} = \frac{\pi^2 \cos\big(\pi(\alpha+\beta+\gamma-1)\big)\Gamma(2\alpha+2\beta+2\gamma-2)}{\cos(\pi\alpha)\Gamma(2\alpha)\cos(\pi\beta)\Gamma(2\beta)\cos(\pi\gamma)\Gamma(2\gamma)} \frac{1}{|t_{12}|^{2\alpha+2\beta+2\gamma-2}}\,. \tag{A.6}$$

Additional similar types of integrals may be found in section 3 of [49]. Notice that the integral (A.2), (A.3) and (A.6) are proportional to $\delta(\tau_{12})$ when $2\alpha+2\beta+2\gamma=3$, similar to those listed in [49]. We omitted these special cases in the above table for simplicity.

These results can be derived from slightly tedious computations building on the basic identities [84]

$$\frac{1}{|t|^{2\Delta}} = \frac{1}{2\cos(\pi\Delta)\Gamma(2\Delta)} \int d\omega\, e^{i\omega t} \frac{1}{|w|^{1-2\Delta}}\,, \tag{A.7}$$

$$\frac{\mathrm{sgn}(t)}{|t|^{2\Delta}} = \frac{1}{2i\sin(\pi\Delta)\Gamma(2\Delta)} \int dw\, e^{iwt} \frac{\mathrm{sgn}(w)}{|w|^{1-2\Delta}}\,. \tag{A.8}$$

Here we provide one example of such a derivation:

$$\int dt\, dt' \frac{\mathrm{sgn}(t_1-t)\,\mathrm{sgn}(t_2-t')\,\mathrm{sgn}(t-t')}{|t_1-t|^{2\alpha}|t_2-t'|^{2\beta}|t-t'|^{2\gamma}} \tag{A.9}$$

$$= \int dt\, dt' \frac{1}{2i\sin(\pi\alpha)\Gamma(2\alpha)} \frac{1}{2i\sin(\pi\beta)\Gamma(2\beta)} \frac{1}{2i\sin(\pi\gamma)\Gamma(2\gamma)} \tag{A.10}$$

$$\times \int dw\, e^{iw(t_1-t)} \frac{\mathrm{sgn}(w)}{|w|^{1-2\alpha}} \int du\, e^{iu(t_2-t')} \frac{\mathrm{sgn}(u)}{|u|^{1-2\beta}} \int dv\, e^{iv(t-t')} \frac{\mathrm{sgn}(v)}{|v|^{1-2\gamma}} \tag{A.11}$$

$$= \frac{(2\pi)}{2i\sin(\pi\alpha)\Gamma(2\alpha)} \frac{1}{2i\sin(\pi\beta)\Gamma(2\beta)} \frac{1}{2i\sin(\pi\gamma)\Gamma(2\gamma)} \tag{A.12}$$

$$\times \int dw \int dt\, e^{i\left(wt_1+ut_2+(-u-w)t\right)} \frac{\mathrm{sgn}(w)}{|w|^{1-2\alpha}} \int du \frac{\mathrm{sgn}(u)}{|u|^{1-2\beta}} \frac{\mathrm{sgn}(-u)}{|u|^{1-2\gamma}} \tag{A.13}$$

$$= \frac{(2\pi)^2}{2i\sin(\pi\alpha)\Gamma(2\alpha)} \frac{1}{2i\sin(\pi\beta)\Gamma(2\beta)} \frac{1}{2i\sin(\pi\gamma)\Gamma(2\gamma)} \tag{A.14}$$

$$\times \int dw\, e^{i(w(t_1-t_2))} \frac{\mathrm{sgn}(w)}{|w|^{1-2\alpha}} \frac{\mathrm{sgn}(-w)}{|w|^{1-2\beta}} \frac{\mathrm{sgn}(w)}{|w|^{1-2\gamma}} \tag{A.15}$$

$$= \frac{\pi^2 \sin\big(\pi(\alpha+\beta+\gamma-1)\big)\Gamma(2\alpha+2\beta+2\gamma-2)}{\sin(\pi\alpha)\Gamma(2\alpha)\sin(\pi\beta)\Gamma(2\beta)\sin(\pi\gamma)\Gamma(2\gamma)} \frac{\mathrm{sgn}(t_{12})}{|t_{12}|^{2\alpha+2\beta+2\gamma-2}}\,. \tag{A.16}$$

References

[1] S. Sachdev and J. Ye, *Gapless spin fluid ground state in a random, quantum Heisenberg magnet*, *Phys. Rev. Lett.* **70** (1993) 3339 [cond-mat/9212030] [INSPIRE].

[2] O. Parcollet and A. Georges, *Non-Fermi-liquid regime of a doped Mott insulator*, *Phys. Rev.* **B 59** (1999) 5341 [cond-mat/9806119].

[3] A. Georges, O. Parcollet and S. Sachdev, *Mean field theory of a quantum Heisenberg spin glass*, *Phys. Rev. Lett.* **85** (2000) 840 [cond-mat/9909239].

[4] A. Kitaev, *Hidden correlations in the Hawking radiation and thermal noise*, KITP seminar, University of California U.S.A. (2015), http://online.kitp.ucsb.edu/online/joint98/kitaev/.

[5] A. Kitaev, *A simple model of quantum holography*, talks given at the *KITP Entanglement Workshop*, University of California U.S.A. (2015), http://online.kitp.ucsb.edu/online/entangled15/kitaev/, http://online.kitp.ucsb.edu/online/entangled15/kitaev2/.

[6] J. Maldacena and D. Stanford, *Remarks on the Sachdev-Ye-Kitaev model*, *Phys. Rev.* **D 94** (2016) 106002 [arXiv:1604.07818] [INSPIRE].

[7] A. Strominger, *AdS_2 quantum gravity and string theory*, *JHEP* **01** (1999) 007 [hep-th/9809027] [INSPIRE].

[8] J.M. Maldacena, J. Michelson and A. Strominger, *Anti-de Sitter fragmentation*, *JHEP* **02** (1999) 011 [hep-th/9812073] [INSPIRE].

[9] S. Sachdev, *Holographic metals and the fractionalized Fermi liquid*, *Phys. Rev. Lett.* **105** (2010) 151602 [arXiv:1006.3794] [INSPIRE].

[10] S.H. Shenker and D. Stanford, *Black holes and the butterfly effect*, *JHEP* **03** (2014) 067 [arXiv:1306.0622] [INSPIRE].

[11] A. Almheiri and J. Polchinski, *Models of AdS_2 backreaction and holography*, *JHEP* **11** (2015) 014 [arXiv:1402.6334] [INSPIRE].

[12] S.H. Shenker and D. Stanford, *Stringy effects in scrambling*, *JHEP* **05** (2015) 132 [arXiv:1412.6087] [INSPIRE].

[13] J. Maldacena, S.H. Shenker and D. Stanford, *A bound on chaos*, *JHEP* **08** (2016) 106 [arXiv:1503.01409] [INSPIRE].

[14] S. Sachdev, *Bekenstein-Hawking entropy and strange metals*, *Phys. Rev.* **X 5** (2015) 041025 [arXiv:1506.05111] [INSPIRE].

[15] M. Blake and A. Donos, *Diffusion and chaos from near AdS_2 horizons*, *JHEP* **02** (2017) 013 [arXiv:1611.09380] [INSPIRE].

[16] J. Maldacena, D. Stanford and Z. Yang, *Diving into traversable wormholes*, *Fortschr. Phys.* **65** (2017) 1700034 [arXiv:1704.05333] [INSPIRE].

[17] D. Bagrets, A. Altland and A. Kamenev, *Sachdev-Ye-Kitaev model as Liouville quantum mechanics*, *Nucl. Phys.* **B 911** (2016) 191 [arXiv:1607.00694] [INSPIRE].

JHEP10(2017)202

[18] D. Stanford and E. Witten, *Fermionic localization of the Schwarzian theory*, *JHEP* **10** (2017) 008 [arXiv:1703.04612] [INSPIRE].

[19] T.G. Mertens, G.J. Turiaci and H.L. Verlinde, *Solving the Schwarzian via the conformal bootstrap*, *JHEP* **08** (2017) 136 [arXiv:1705.08408] [INSPIRE].

[20] J. Maldacena, D. Stanford and Z. Yang, *Conformal symmetry and its breaking in two dimensional nearly anti-de Sitter space*, *Prog. Theor. Exp. Phys.* **2016** (2016) 12C104 [arXiv:1606.01857] [INSPIRE].

[21] J. Engelsöy, T.G. Mertens and H. Verlinde, *An investigation of AdS_2 backreaction and holography*, *JHEP* **07** (2016) 139 [arXiv:1606.03438] [INSPIRE].

[22] M. Cvetič and I. Papadimitriou, *AdS_2 holographic dictionary*, *JHEP* **12** (2016) 008 [*Erratum ibid.* **01** (2017) 120] [arXiv:1608.07018] [INSPIRE].

[23] S. Förste and I. Golla, *Nearly AdS_2 SUGRA and the super-Schwarzian*, *Phys. Lett.* **B 771** (2017) 157 [arXiv:1703.10969] [INSPIRE].

[24] J. Polchinski and V. Rosenhaus, *The spectrum in the Sachdev-Ye-Kitaev model*, *JHEP* **04** (2016) 001 [arXiv:1601.06768] [INSPIRE].

[25] A. Jevicki, K. Suzuki and J. Yoon, *Bi-local holography in the SYK model*, *JHEP* **07** (2016) 007 [arXiv:1603.06246] [INSPIRE].

[26] A. Jevicki and K. Suzuki, *Bi-local holography in the SYK model: perturbations*, *JHEP* **11** (2016) 046 [arXiv:1608.07567] [INSPIRE].

[27] A.M. García-García and J.J.M. Verbaarschot, *Spectral and thermodynamic properties of the Sachdev-Ye-Kitaev model*, *Phys. Rev.* **D 94** (2016) 126010 [arXiv:1610.03816] [INSPIRE].

[28] J.S. Cotler et al., *Black holes and random matrices*, *JHEP* **05** (2017) 118 [arXiv:1611.04650] [INSPIRE].

[29] Y. Liu, M.A. Nowak and I. Zahed, *Disorder in the Sachdev-Yee-Kitaev model*, *Phys. Lett.* **B 773** (2017) 647 [arXiv:1612.05233] [INSPIRE].

[30] A.M. García-García and J.J.M. Verbaarschot, *Analytical spectral density of the Sachdev-Ye-Kitaev model at finite N*, *Phys. Rev.* **D 96** (2017) 066012 [arXiv:1701.06593] [INSPIRE].

[31] T. Li, J. Liu, Y. Xin and Y. Zhou, *Supersymmetric SYK model and random matrix theory*, *JHEP* **06** (2017) 111 [arXiv:1702.01738] [INSPIRE].

[32] D.J. Gross and V. Rosenhaus, *The bulk dual of SYK: cubic couplings*, *JHEP* **05** (2017) 092 [arXiv:1702.08016] [INSPIRE].

[33] R. Gurau, *The complete $1/N$ expansion of colored tensor models in arbitrary dimension*, *Ann. Henri Poincaré* **13** (2012) 399 [arXiv:1102.5759] [INSPIRE].

[34] V. Bonzom, R. Gurau, A. Riello and V. Rivasseau, *Critical behavior of colored tensor models in the large N limit*, *Nucl. Phys.* **B 853** (2011) 174 [arXiv:1105.3122] [INSPIRE].

[35] V. Bonzom, R. Gurau and V. Rivasseau, *Random tensor models in the large N limit: uncoloring the colored tensor models*, *Phys. Rev.* **D 85** (2012) 084037 [arXiv:1202.3637] [INSPIRE].

[36] S. Carrozza and A. Tanasa, *$O(N)$ random tensor models*, *Lett. Math. Phys.* **106** (2016) 1531 [arXiv:1512.06718] [INSPIRE].

JHEP10(2017)202

[37] E. Witten, *An SYK-like model without disorder*, arXiv:1610.09758 [INSPIRE].

[38] R. Gurau, *The complete $1/N$ expansion of a SYK-like tensor model*, *Nucl. Phys.* **B 916** (2017) 386 [arXiv:1611.04032] [INSPIRE].

[39] I.R. Klebanov and G. Tarnopolsky, *Uncolored random tensors, melon diagrams and the Sachdev-Ye-Kitaev models*, *Phys. Rev.* **D 95** (2017) 046004 [arXiv:1611.08915] [INSPIRE].

[40] T. Nishinaka and S. Terashima, *A note on Sachdev-Ye-Kitaev like model without random coupling*, arXiv:1611.10290 [INSPIRE].

[41] C. Peng, M. Spradlin and A. Volovich, *A supersymmetric SYK-like tensor model*, *JHEP* **05** (2017) 062 [arXiv:1612.03851] [INSPIRE].

[42] C. Krishnan, S. Sanyal and P.N. Bala Subramanian, *Quantum chaos and holographic tensor models*, *JHEP* **03** (2017) 056 [arXiv:1612.06330] [INSPIRE].

[43] R. Gurau, *Quenched equals annealed at leading order in the colored SYK model*, arXiv:1702.04228 [INSPIRE].

[44] V. Bonzom, L. Lionni and A. Tanasa, *Diagrammatics of a colored SYK model and of an SYK-like tensor model, leading and next-to-leading orders*, *J. Math. Phys.* **58** (2017) 052301 [arXiv:1702.06944] [INSPIRE].

[45] C. Krishnan, K.V.P. Kumar and S. Sanyal, *Random matrices and holographic tensor models*, *JHEP* **06** (2017) 036 [arXiv:1703.08155] [INSPIRE].

[46] P. Narayan and J. Yoon, *SYK-like tensor models on the lattice*, *JHEP* **08** (2017) 083 [arXiv:1705.01554] [INSPIRE].

[47] I.R. Klebanov and G. Tarnopolsky, *On large N limit of symmetric traceless tensor models*, *JHEP* **10** (2017) 037 [arXiv:1706.00839] [INSPIRE].

[48] A. Mironov and A. Morozov, *Correlators in tensor models from character calculus*, *Phys. Lett.* **B 774** (2017) 210 [arXiv:1706.03667] [INSPIRE].

[49] C. Peng, *Vector models and generalized SYK models*, *JHEP* **05** (2017) 129 [arXiv:1704.04223] [INSPIRE].

[50] D.J. Gross and V. Rosenhaus, *A generalization of Sachdev-Ye-Kitaev*, *JHEP* **02** (2017) 093 [arXiv:1610.01569] [INSPIRE].

[51] Y. Gu, X.-L. Qi and D. Stanford, *Local criticality, diffusion and chaos in generalized Sachdev-Ye-Kitaev models*, *JHEP* **05** (2017) 125 [arXiv:1609.07832] [INSPIRE].

[52] M. Berkooz, P. Narayan, M. Rozali and J. Simón, *Higher dimensional generalizations of the SYK model*, *JHEP* **01** (2017) 138 [arXiv:1610.02422] [INSPIRE].

[53] G. Turiaci and H. Verlinde, *Towards a 2d QFT analog of the SYK model*, arXiv:1701.00528 [INSPIRE].

[54] Y. Gu, A. Lucas and X.-L. Qi, *Energy diffusion and the butterfly effect in inhomogeneous Sachdev-Ye-Kitaev chains*, *SciPost Phys.* **2** (2017) 018 [arXiv:1702.08462] [INSPIRE].

[55] S.-K. Jian and H. Yao, *Solvable SYK models in higher dimensions: a new type of many-body localization transition*, arXiv:1703.02051 [INSPIRE].

[56] S.R. Das, A. Jevicki and K. Suzuki, *Three dimensional view of the SYK/AdS duality*, *JHEP* **09** (2017) 017 [arXiv:1704.07208] [INSPIRE].

JHEP10(2017)202

[57] Y.-Z. You, A.W.W. Ludwig and C. Xu, *Sachdev-Ye-Kitaev model and thermalization on the boundary of many-body localized fermionic symmetry-protected topological states*, *Phys. Rev.* **B 95** (2017) 115150 [arXiv:1602.06964] [INSPIRE].

[58] W. Fu and S. Sachdev, *Numerical study of fermion and boson models with infinite-range random interactions*, *Phys. Rev.* **B 94** (2016) 035135 [arXiv:1603.05246] [INSPIRE].

[59] I. Danshita, M. Hanada and M. Tezuka, *Creating and probing the Sachdev-Ye-Kitaev model with ultracold gases: towards experimental studies of quantum gravity*, *Prog. Theor. Exp. Phys.* **2017** (2017) 083I01 [arXiv:1606.02454] [INSPIRE].

[60] L. García-Álvarez et al., *Digital quantum simulation of minimal AdS/CFT*, *Phys. Rev. Lett.* **119** (2017) 040501 [arXiv:1607.08560] [INSPIRE].

[61] S. Banerjee and E. Altman, *Solvable model for a dynamical quantum phase transition from fast to slow scrambling*, *Phys. Rev.* **B 95** (2017) 134302 [arXiv:1610.04619] [INSPIRE].

[62] R.A. Davison et al., *Thermoelectric transport in disordered metals without quasiparticles: the Sachdev-Ye-Kitaev models and holography*, *Phys. Rev.* **B 95** (2017) 155131 [arXiv:1612.00849] [INSPIRE].

[63] S.A. Hartnoll, A. Lucas and S. Sachdev, *Holographic quantum matter*, arXiv:1612.07324 [INSPIRE].

[64] Z. Bi, C.-M. Jian, Y.-Z. You, K.A. Pawlak and C. Xu, *Instability of the non-Fermi liquid state of the Sachdev-Ye-Kitaev model*, *Phys. Rev.* **B 95** (2017) 205105 [arXiv:1701.07081] [INSPIRE].

[65] C.-M. Jian, Z. Bi and C. Xu, *A model for continuous thermal metal to insulator transition*, *Phys. Rev.* **B 96** (2017) 115122 [arXiv:1703.07793] [INSPIRE].

[66] X.-Y. Song, C.-M. Jian and L. Balents, *A strongly correlated metal built from Sachdev-Ye-Kitaev models*, arXiv:1705.00117 [INSPIRE].

[67] S.-F. Wu, B. Wang, X.-H. Ge and Y. Tian, *Universal diffusion in holography*, arXiv:1706.00718 [INSPIRE].

[68] K. Jensen, *Chaos in AdS_2 holography*, *Phys. Rev. Lett.* **117** (2016) 111601 [arXiv:1605.06098] [INSPIRE].

[69] F. Ferrari, *The large D limit of planar diagrams*, arXiv:1701.01171 [INSPIRE].

[70] W.W. Ho and D. Radičević, *The ergodicity landscape of quantum theories*, arXiv:1701.08777 [INSPIRE].

[71] M. Berkooz, P. Narayan, M. Rozali and J. Simón, *Comments on the random Thirring model*, *JHEP* **09** (2017) 057 [arXiv:1702.05105] [INSPIRE].

[72] J.S. Cotler, G.R. Penington and D.H. Ranard, *Locality from the spectrum*, arXiv:1702.06142 [INSPIRE].

[73] D. Bagrets, A. Altland and A. Kamenev, *Power-law out of time order correlation functions in the SYK model*, *Nucl. Phys.* **B 921** (2017) 727 [arXiv:1702.08902] [INSPIRE].

[74] P. Caputa, N. Kundu, M. Miyaji, T. Takayanagi and K. Watanabe, *Anti-de Sitter space from optimization of path integrals in conformal field theories*, *Phys. Rev. Lett.* **119** (2017) 071602 [arXiv:1703.00456] [INSPIRE].

[75] D. Chowdhury and B. Swingle, *Onset of many-body chaos in the $O(N)$ model*, *Phys. Rev.* **D 96** (2017) 065005 [arXiv:1703.02545] [INSPIRE].

JHEP10(2017)202

[76] H. Itoyama, A. Mironov and A. Morozov, *Rainbow tensor model with enhanced symmetry and extreme melonic dominance*, *Phys. Lett.* **B 771** (2017) 180 [arXiv:1703.04983] [INSPIRE].

[77] H. Itoyama, A. Mironov and A. Morozov, *Ward identities and combinatorics of rainbow tensor models*, *JHEP* **06** (2017) 115 [arXiv:1704.08648] [INSPIRE].

[78] M. Blake, R.A. Davison and S. Sachdev, *Thermal diffusivity and chaos in metals without quasiparticles*, arXiv:1705.07896 [INSPIRE].

[79] R. Gurau, *The $\imath\epsilon$ prescription in the SYK model*, arXiv:1705.08581 [INSPIRE].

[80] S. Dartois, H. Erbin and S. Mondal, *Conformality of $1/N$ corrections in SYK-like models*, arXiv:1706.00412 [INSPIRE].

[81] T. Kanazawa and T. Wettig, *Complete random matrix classification of SYK models with $\mathcal{N} = 0$, 1 and 2 supersymmetry*, *JHEP* **09** (2017) 050 [arXiv:1706.03044] [INSPIRE].

[82] R. Gurau, *The $1/N$ expansion of tensor models with two symmetric tensors*, arXiv:1706.05328 [INSPIRE].

[83] C. Krishnan and K.V.P. Kumar, *Towards a finite-N hologram*, arXiv:1706.05364 [INSPIRE].

[84] W. Fu, D. Gaiotto, J. Maldacena and S. Sachdev, *Supersymmetric Sachdev-Ye-Kitaev models*, *Phys. Rev.* **D 95** (2017) 026009 [*Addendum ibid.* **D 95** (2017) 069904] [arXiv:1610.08917] [INSPIRE].

[85] D. Anninos, T. Anous and F. Denef, *Disordered quivers and cold horizons*, *JHEP* **12** (2016) 071 [arXiv:1603.00453] [INSPIRE].

[86] N. Sannomiya, H. Katsura and Y. Nakayama, *Supersymmetry breaking and Nambu-Goldstone fermions with cubic dispersion*, *Phys. Rev.* **D 95** (2017) 065001 [arXiv:1612.02285] [INSPIRE].

[87] J. Murugan, D. Stanford and E. Witten, *More on supersymmetric and 2d analogs of the SYK model*, *JHEP* **08** (2017) 146 [arXiv:1706.05362] [INSPIRE].

[88] J. Yoon, *Supersymmetric SYK model: bi-local collective superfield/supermatrix formulation*, arXiv:1706.05914 [INSPIRE].

[89] K. Bulycheva, *A note on the SYK model with complex fermions*, arXiv:1706.07411 [INSPIRE].

JHEP10(2017)202